JC10 Rec'd PCT/PTO 17 DEC 2001

FORMS PTO-1390 (REV 10-96) U.S. DEPARTMENT OF COMMERCE PATENT AND TRADEMARK OFFICE

TRANSMITTAL LETTER TO THE UNITED STATES DESIGNATED/ELECTED OFFICE (DO/EO/US) CONCERNING A FILING UNDER 35 U.S.C. 371

ATTORNEY'S DOCKET NUMBER	
SI01-030	
U.S. APPLICATION NO. (If known, see 37 CFR 1.5)	
TBA 10/018863	
INTERNATIONAL APPLICATION NO.	INTERNATIONAL FILING DATE
PCT/DE00/02008	June 16, 2000
PRIORITY DATE CLAIMED	
June 16, 1999	

TITLE OF INVENTION

BERECHNUNG DER SPLEISSDÄMPFUNG NACH MESSUNG DER GEOMETRIE (METHODS FOR DETERMINING THE ATTENUATION OF A SPLICE THAT CONNECTS TWO OPTICAL WAVEGUIDES)

APPLICANT(S) FOR DO/EO/US

Corning Incorporated

Applicant herewith submits to the United States Designated/Elected Office (DO/EO/US) the following items and other information:

1. ☒ This is a **FIRST** submission of items concerning a filing under 35 U.S.C. 371.
2. ☐ This is a **SECOND** or **SUBSEQUENT** submission of items concerning a filing under 35 U.S.C.371.
3. ☐ This express request to being national examination procedures (35 U.S.C. 371(f)) at any time rather than delay examination until the expiration of the applicable time limit set in 35 U.S.C. 371(b) and PCT Articles 22 and 39(1).
4. ☒ A proper Demand for International Preliminary Examination was made by the 19th month from the earliest claimed priority date.
5. ☒ A copy of the International Application as filed (35 U.S.C. 371(c)(2))
   a. ☐ is transmitted herewith (required only if not transmitted by the International Bureau).
   b. ☒ has been transmitted by the International Bureau.
   c. ☐ is not required, as the application was filed in the United States Receiving Office (RO/US).
6. ☐ A translation of the International Application into English (35 U.S.C. 371(c)(2)).
7. ☒ Amendments to the claims of the International Application under PCT Article 19 (35 U.S.C. 371(c)(3)).
   a. ☐ are transmitted herewith (required only if not transmitted by the International Bureau).
   b. ☐ have been transmitted by the International Bureau.
   c. ☒ have not been made; however, the time limit for making such amendments has NOT expired.
   d. ☐ have not been made and will not be made.
8. ☐ A translation of the amendments to the claims under PCT Article 19 (35 U.S.C. 371(c)(3)).
9. ☒ An oath or declaration of the inventor(s) (35 U.S.C. 371(c)(4)).
10. ☐ A translation of the annexes to the International Preliminary Examination Report under PCT Article 36 (35 U.S.C. 371(c)(5)).

Items 11. To 16. Below concern document(s) or information included:

11. ☒ An Information Disclosure Statement under 37 CFR 1.97 and 1.98.
12. ☒ An Assignment document for recording. A separate cover sheet in compliance with 37 CFR 3.28 and 3.31 is included.
13. ☒ A FIRST preliminary amendment.
14. ☐ A SECOND or SUBSEQUENT preliminary amendment.
15. ☐ A change of power of attorney and/or address letter.
16. ☐ Other items or information:

U.S. APPLICATION NO. (if known, see 37 CFR 1.5)	INTERNATIONAL APPLICATION NO.	ATTORNEY'S DOCKET NUMBER
TBA 10/018863	PCT/DE00/02008	SI01-030

17. ☒ The following fees are submitted:

	CALCULATIONS	PTO USE ONLY
BASIC NATIONAL FEE (37 CFR 1.492 (a)(1)-(5): Neither international preliminary examination fee (37 DFR 1.482) nor international search fee (37 CFR 1.445(a)(2)) paid to USPTO and International Search Report not prepared by the EPO or JPO ..... **$1040.00** International preliminary examination fee (37 CFR 1.482) not paid to USPTO but International Search Report prepared by the EPO or JPO ..... **$890.00** International preliminary examination fee (37 CFR 1.482) not paid to USPTO but international search fee (37 CFR 1.445(a)(2)) paid to USPTO ..... **$740.00** International preliminary examination fee paid to USPTO (37 CFR 1.482) but all claims did not satisfy provisions of PCT Article 33 (1)-(4) ..... **$710.00** International preliminary examination fee paid to USPTO (37 CFR 1.482) and all claims satisfied provisions of PCT Article 33(1)-(4) **$100.00**		
ENTER APPROPRIATE BASIC FEE AMOUNT =	**$890.00**	
Surcharge of **$130.00** for furnishing the oath or declaration later than ☐ 20 ☐ 30 months from the earliest claimed priority date (37 CFR 1.492(e)).	$	

CLAIMS	NUMBER FILED	NUMBER EXTRA	RATE	
Total claims	18 - 20 =	0	X $18.00	$.00
Independent claims	1 - 3 =	0	X $84.00	$.00
MULTIPLE DEPENDANT CLAIM(S) (if applicable)			+ $270.00	$.00
TOTAL OF ABOVE CALCULATIONS =				$.00
Reduction of ½ for filing by small entity, if applicable. Verified Small Entity Statement must also be filed (Note 37 CFR 1.9, 1.27, 1.28) +				$
SUBTOTAL =				$890.00
Processing fee of **$130.00** for furnishing the English translation later than ☐ 20 ☒ 30 months from the earliest claimed priority date (37 CFR 1.492(f)). +				$ 130.00
TOTAL NATIONAL FEE =				$1,020.00
Fee for recording the enclosed assignment (37 CFR 1.21(h)). The assignment must be accompanied by an appropriate cover sheet (37 CFR 3.28, 3.31). **$40.00** per property +				$ 40.00
TOTAL FEES ENCLOSED =				$.00
			Amount to be refunded:	$
			Charged:	**$1,060.00**

I hereby certify that this paper or fee is being deposited with the United States Postal Service "Express Mail Post Office to Addressee" service under 37 CFR 1.10 on the date indicated below and is Addressed to the Commissioner of Patents and Trademarks, Washington, DC 20231

on 12-17-01 (Date) By: Walter M Douglas (Signature)

"EXPRESS MAIL" Mailing Label No. EV044147027SUS

a. ☐ A check in the amount of $ _____ to cover the above fees is enclosed.

b. ☒ Corning Incorporated hereby authorizes use of **Deposit Account No. 03-3325** in the amount of **$1,060.00** to cover the above fees.

c. ☒ The Commissioner is hereby authorized to charge any additional fees which may be required, or credit any overpayment to Deposit Account No. 03-3325.

NOTE: Where an appropriate time limit under 37 CFR 1.494 or 1.495 has not been met, a petition to revive (37 CFR 1.137(a) or (b)) must be filed and granted to restore the application to pending status.

Send all correspondence to:
Walter M. Douglas
Corning Incorporated
SP-TI-03
Corning, NY 14831

Walter M Douglas
Signature

Registration No.: 34,510
(607) 974-2431

#5

IN THE UNITED STATES PATENT AND TRADEMARK OFFICE

PCT APPLICATION

Inventor:	Bert Zamzow	
Serial No:	10/018,863	Group Art Unit: TBA
Filing Date:	12/17/01	Examiner: TBA
Title:	CALCULATING SPLICE LOSS BY GEOMETRIC MEASUREMENT	

Commissioner for Patents
Box PCT
United States Patent and Trademark Office
Washington, DC 20231

RESPONSE AND SECOND PRELIMINARY AMENDMENT

This paper is submitted in response to the Notification of Missing Requirements under 35 U.S.C. 371, mailed March 1, 2002 and having a period for response set to expire on May 1, 2002. The Notice is directed to applicants having to supply an English translation of the application. A verified translation of the application as it was filed is enclosed. Please enter the following amendments before any action on the merits.

In the Specification

Please see attached application entitled "Clean Version of Amended Application". Please also see "Remarks".

In the Claims

Please see attached application entitled "Clean Version of Amended Application". Please also see "Remarks".

In the Abstract

Please see attached application entitled "Clean Version of Amended Application". Please also see "Remarks".

Remarks

The Notification of Missing Requirements under 35 U.S.C. 371, mailed March 1, 2002 requires the submission of an English translation of the application as filed and a translation of the substitute claims filed in German in the Preliminary Amendment submitted on December 17, 2001. Enclosed with this second preliminary amendment are the following:

1. A translation of the application as filed with the translator's Verification of Translation letter attached. This translation contains the original Claims 1-10, which were cancelled by the Preliminary Amendment filed with the application on December 17, 2001.
2. A translation of the substitute claims 11-28, which were added, in German, by the Preliminary Amendment filed on December 17, 2001.
3. A marked-up, translated application showing amendments made to conform to the formalities of U.S. filing requirements. This application is entitled "Version with Markings to Show Changes Made". The application in marked-up form shows:
   (a) all amendments made to the application to bring it into conformity to U.S. practice;
   (b) the deletion of original claims 1-10;
   (c) all the amendments made to the translated claims 11-28; and
   (d) the insertion of the Abstract Of The Invention.
4. A clean copy of the translated application, which includes amendments made and which contains amended claims 11-28. This application is entitled " Clean Version of Amended Application". Please use this clean version of the application for examination purposes.
5. The required fee of $130.00.

In the applications referenced in numbers 3 and 4 above, section headings (Summary of the Invention, Detailed Description, etc.) have been added or the wording changed from the translated document, grammatical and typographical errors were corrected, a claim to the priority of first filed German application and the PCT

application has been inserted, and awkward phrasing was changed and lengthy sentences were broken into two sentences to make the application more readable in English. Referring now to the Verified Translation, one particular change applicants wish to point out is that the second and third paragraphs of the Section 3 of the Verified Translation, titled "Subject matter, goals and advantages of the invention", were moved to become the first two paragraphs of the Detailed Description of The Invention.

As referenced above, a translation of claims 11-28, which were filed in the German language by a Preliminary Amendment accompanying the Patent Application filed on December 17, 2001, is enclosed. The German language claims 11-28 were prepared by applicants' undersigned attorney and were based on the originally filed German claims, amended to remove the multiple dependencies permitted in European practice generally. For example, where the original German claim 3 was dependent on "claims 1 and 2", in the Preliminary Amendment, this claim was made into claims 13 and 14 which are dependent on claims 11 and 12, respectively. The same practice was carried out for all claims 11-28. No new subject matter was added.

Applicants' undersigned attorney also prepared the English translation of the German claims 11-28.

By his signature given below, the undersigned attorney for applicant does hereby declare that all statements made herein of his own knowledge are true and that all statements made on information and belief are believed to be true; and further that these statements are made with the knowledge that willful false statements and the like so made are punishable by fine, imprisonment or both, under Section 1 of Title 18 of the United States Code and that such willful false statements may jeopardize the validity of any patents issued upon this application.

Authorization by Corning Incorporated is given to charge the above noted fee of $130.00 and any additional fees necessary due in connection with this filing to Deposit Account No. 03-3325.

If there are any questions, please contact the undersigned attorney for applicant.

Respectfully submitted,

CORNING INCORPORATED

Date: April 5, 2002

Walter M. Douglas
Registration No. 34,510
Corning Incorporated
Patent Department
Mail Stop SP-TI-03-1
Corning, NY 14831

CERTIFICATE OF MAILING UNDER 37 C.F.R. § 1.8: I hereby certify that this correspondence is being deposited with the United States Postal Service as first class mail in an envelope addressed to Asst. Commissioner of Patents and Trademarks, Washington, D.C. 20231 on

April 5, 2002
Date of Deposit

Walter M. Douglas
Name of applicant, assignee, or
Registered Representative

Signature

April 5, 2002
Date of Signature

Version with Markings to Show Changes Made

SI01-030

~~Description~~

CALCULATING SPLICE LOSS BY GEOMETRIC MEASUREMENT

Cross-Reference To Related Applications

This application claims the benefit of priority under 35 U.S.C. § 119 of German Patent Application No. 19927583.1 filed June 16, 1999, and is a national stage filing under 35 U.S.C. § 371 of PCT Application PCT/DE00/02008, filed June 16, 2000.

Field of The Invention

The invention is directed to optical waveguides, and in particular to methods for determining the attenuation of a splice connecting two optical waveguides. The splice attenuation is calculated from the intensity values assigned to field distributions, before and after the splice, corresponding to a mode that is capable of propagating in the fiber.

~~**1. Introduction**~~

Background Of The Invention

The method known as "thermal splicing" can be used to interconnect both monomode and multimode glass fibers and glass fiber strips in a bonded, low-loss and permanent fashion. Since the costs of constructing an optical waveguide cable network are not inconsiderably influenced by splicing as a work step that is frequently to be carried out, convenient devices which can also be used on site under difficult conditions have been developed which execute all the steps required for welding glass fibers in a largely fully automatic fashion (see ICCS and Future-Link; catalog 1998; Siemens-Communication-Cable Networks; pages 107 - 116 ~~[1], for example~~). The loss in the splice junction produced in such a device is a function, inter alia, of the exact alignment of the optically conducting fiber cores, the quality of the fiber end faces (roughness, angle of fracture, etc) and of the welding parameters (welding time, welding current) selected by the operator or described by the respective control program.

~~**2. Prior art**~~

Disturbances in the geometry of the optically conducting fiber core are decisive for the magnitude of the loss in the splice produced. In particular, the ~~The~~ loss caused ~~in particular~~ by a core offset, bending of the core or widening or

Version with Markings to Show Changes Made

tapering of the core can be determined, for example, by means of a transmission measurement and the use of a bending coupler (LID system) installed in the splicer. In this case, light is coupled into the glass fiber upstream of the splice point, and coupled out again downstream of the splice point. The intensity of the light transmitted from one glass fiber into the other glass fiber via the splice is then a measure of the loss. This measurement method cannot be applied, however, when an excessively thick or dark-colored fiber coating prevents light from being coupled into and out of the fiber core.

The method disclosed in EP 0 326 988 B1 ~~[2]~~ for determining the splice loss is based on the optical detection of the core offset, the oblique position of the fiber cores and the core bending in the region of the splice point. An empirically determined formula describes the functional dependence of the loss on the said parameters. Since the method does not require light to be coupled into and out of the fiber core, it can always be applied independently of the light-passing capability of the fiber coating. However, it supplies reliable loss values only when the previously named parameters alone determine the loss of the splice. However, this is not always the case, particularly with wrongly set welding parameters or high losses.

~~**3. Subject matter, goals and advantages of the invention**~~

Summary of The Invention

The ~~subject matter of the~~ invention is directed to a method for determining the loss in ~~of~~ a splice connecting two optical waveguides. The term "splice" in this case denotes that bonded connection, in particular produced by thermal fusing/welding, between at least two optically conducting structures or elements, that is to say, in particular, the connection between glass fibers, glass fiber strips/ glass fiber bundles or the connection between a glass fiber or a glass fiber strip and an active or passive optical component.

~~The method is intended to enable the user to determine the loss in the splice produced, doing so with high accuracy while taking account of all the parameters substantially influencing the loss. This object is achieved by means of a method having the features specified in patent claim 1. The dependent claims relate to advantageous embodiments and developments of the method.~~

Version with Markings to Show Changes Made

~~The proposed method can be applied straight away in a modern splicer, since all that is needed is to adapt its software appropriately. The method is distinguished, furthermore, by the following properties:~~

~~——— the achievable accuracy of the determination of loss is limited essentially only by the quality of the optical system serving to visualize the fiber core, and the performance of the processor executing the field calculation;~~

~~——— the loss in the splice can be determined as a function of direction;~~

~~——— comparatively thick and/or darkly colored fiber coatings cannot impair the measurement;~~

~~——— the splice loss can be calculated for any desired operating wavelength, and~~

~~——— the method permits simple adaptation to the respective requirements (for example high accuracy, fast measurement).~~

~~**4. Drawings**~~

Brief Description Of The Drawings

The invention is explained in more detail below with the aid of drawings, in which:

Fig.~~ure~~ 1 ~~——~~shows the schematic structure of a modern thermal splicer operating largely fully automatically;

Fig.~~ure~~ 2 ~~——~~illustrates ~~shows~~ the relative position of the ends of two optical fibers that are to be connected;

a) after being brought together and coarsely positioned;

b) after being aligned with reference to their outer contours, and

c) after being aligned with reference to their optically conducting fiber cores;

Fig.~~ure~~ 3 ~~——~~shows the schematic structure of a glass fiber, and the profile n(r) of the refractive index in the plane oriented perpendicular to the fiber longitudinal axis;

Fig.~~ure~~ 4 illustrates ~~————~~shows the intensity distribution ("shadow image" of the glass fiber) produced in the case of transverse transillumination of a glass fiber, by means of an imaging optical system in the sensor plane of a CCD camera;

Fig.~~ure~~ 5 illustrates ~~————~~shows the shadow image of the glass fiber whose core has a lateral offset in the region of the splice;

Fig.~~ure~~ 6 illustrates ~~————~~shows the shadow image of a glass fiber whose core is bent in the region of the splice;

Version with Markings to Show Changes Made

Fig.~~ure~~ 7 illustrates~~——~~ ~~shows~~ the shadow image of a glass fiber whose core is expanded/compressed in the region of the splice,~~;~~

Fig.~~ure~~ 8 illustrates~~——~~ ~~shows~~ the shadow image of a glass fiber in the case of which, because of the diffusion of the dopant atoms, the pair of lines defining the core exhibit a lesser brightness or a lesser contrast in the region of the splice than outside the heating zone,~~; and~~

Fig.~~ure~~ 9 illustrates~~——~~ ~~shows~~ the subdivision into cuboids and layers of the space on which the method of field calculation is based and containing the fiber core.

~~**5. Description of the exemplary embodiments**~~

Detailed Description of The Invention

The method is intended to enable the user to determine the loss in the splice produced, doing so with high accuracy while taking account of all the parameters substantially influencing the loss. This object is achieved by means of a method having the features specified in patent claim 1. The dependent claims relate to advantageous embodiments and developments of the method.

The proposed method can be applied straight away in a modern splicer, since all that is needed is to adapt its software appropriately. The method is distinguished, furthermore, by the following properties:

- the achievable accuracy of the determination of loss is limited essentially only by the quality of the optical system serving to visualize the fiber core and the performance of the processor executing the field calculation;
- the loss in the splice can be determined as a function of direction;
- comparatively thick and/or darkly colored fiber coatings cannot impair the measurement;
- the splice loss can be calculated for any desired operating wavelength, and
- the method permits simple adaptation to the respective requirements (for example high accuracy, fast measurement).

The splicer illustrated only schematically in Fig.~~figure~~ 1 permits optical fibers to be welded in a largely fully automatic fashion. The bonded connection of the optical fibers that is produced with the aid of an arc (electric glow discharge) struck between two electrodes, which is denoted below as "splice" for short, is free of inclusions, the loss caused by the splice being on average approximately L = 0.02 -0.03 dB (identical standard monomode glass fibers).

Version with Markings to Show Changes Made

The connection of the monomode or multimode glass fibers consisting in each case of a core (refractive index n_{core}), a cladding (refractive index $n_{cladding} < n_{core}$) and a coating of one or more layers is usually performed by executing the following method steps:

a) preparing the fiber ends 1/2, that is to say carefully removing the fiber coating, cleaning the fiber ends 1/2 and breaking the fibers in such a way that the fiber end faces are orientated approximately perpendicular to the fiber longitudinal axis (angle of fracture < 0.8°; typically 0.5°);

b) fixing the fiber ends 1/2 in the holders of the splicer;

c) bringing the fiber ends 1/2 together and aligning them by means of high-precision positioning units 3/4/5 by using the LID system 6/7 (Local Injection and Detection) and/or by video image evaluation;

d) cleaning the fiber end faces by briefly heating the fiber ends 1/2;

e) feeding the fiber ends 1/2 and fusing them by striking an electric arc between two electrodes 8/9 arranged in the region of the fiber ends 1/2, and

f) checking the quality of the splice (measuring the splice loss, checking the tensile strength).

Whereas the method steps a) and b) must be executed by the operator, that is to say still have to be done manually, the method steps specified under c) to f) and mentioned further in Catalog 1998 cited above, [1], in particular the determination of the angle of fracture, the quality and the level of contamination of the fiber end faces run under program control in the splicer.

Referring now to Fig. 1, the ~~The~~ splicer is equipped with the following components and elements in order to carry out these method steps:

- —three positioning units 3, 4, and 5 ~~3/4/5~~ for independently displacing the fiber ends 1/2, respectively guided in V grooves, in three orthogonal spatial directions (x-, y- and z-axis ≡ fiber longitudinal axis),
- —a control unit 10 for driving the actuating elements (positioning motors, piezoelectric actuators) of the positioning units 3, 4 and ~~5~~3/4/5,
- —a transmission measuring device consisting of an optical transmitter 6 (light-emitting diode, bending coupler) and an optical receiver 7 (bending coupler, photodiode, amplifier) (LID system, ~~see~~ see Catalog 1998 cited above[1], ~~for example~~),

Version with Markings to Show Changes Made

• —two optical systems for projecting the outer contours or the profile of the two fiber ends 1/2 into two planes (x/z- or y/z-plane) orientated orthogonally relative to one another, the optical systems respectively have a light source 11/12 (light-emitting diode), an imaging optical system 13/14 and a CCD camera 16/17 which is connected to the video evaluating unit 15 and defines the x/z or the y/z sensor plane,

• —a heat source for heating the fiber ends 1/2 to the melting temperature, situated in the region between approximately 1600-2000°C, the supply of heat being performed in the exemplary embodiment shown by means of a glow discharge produced between two electrodes 8/9 and controlled by the unit 18,

• —a central controller 19 which is connected on the input side to the video evaluating unit 15 and executes and monitors all the steps required for splicing in accordance with the selected program, and

• —an LCD monitor (not illustrated).

After the glass fibers have been inserted into the holder of the splicer, their ends 1/2 are not generally aligned opposite one another. As illustrated in Fig. ~~figure~~ 2 schematically in side view, both the outer contours of the fiber ends 1/2 and the fiber cores C1/C2 then do not necessarily exhibit a transverse offset δ_k or δ_c of the same size. The offset δ_k of the outer contours is now measured by evaluating the projections, recorded with the aid of the two CCD cameras 16/17, of the fiber ends 1/2 in the x/z-plane or the y/z-plane. Subsequently, the fiber ends 1/2 are displaced with the aid of the first positioning units 3, 4 and 5 ~~3/4/5~~, driven with the aid of the control unit 10, in a transverse direction, that is to say in the direction of the x- and y-axes until the outer contours of the fiber ends 1/2 are aligned, their transverse offset δ_k thus vanishing at least approximately ($\delta_{kx} \approx \delta_{ky} \approx 0$) both in the x- and in the y-directions. After this alignment, referred to as fine positioning, the fiber ends 1/2 are situated opposite one another, as illustrated in Fig. ~~figure~~ 2b. The core offset δ_c, caused by the eccentric position of the fiber cores C1/C2, which is still present is clearly to be seen.

In order to produce a splice with the lowest possible loss, the fiber ends 1/2 must therefore further be aligned with regard to their cores C1/C2, that is to say the core offset δ_c must be removed or at least minimized. This is performed by using the LID system, which feeds the IR radiation, emitted by a light-emitting diode on the transmitter 6, of wavelength 800 nm $\leq \lambda \leq$ 1600 nm, in particular λ = 1300 nm or λ = 1550 nm, into the left-hand glass fiber via the assigned bending coupler, and measures the intensity of the radiation, coupled from the left-hand fiber end 1 into

Version with Markings to Show Changes Made

the right-hand fiber end 2, by means of the optical receiver, consisting of a second bending coupler and a photodiode amplifier unit. The fiber ends 1/2 are displaced in this case in the transverse direction until the radiation intensity measured in the optical receiver 7 of the LID system reaches a maximum, the fiber ends 1/2 thereby assuming the position illustrated in Fig. ~~figure~~ 2c (fiber cores C1/C2 in line and aligned in parallel with the z-axis; small contour offset corresponding to the corrected core offset δ_c).

Subsequently, the fiber ends 1/2 are heated by striking the electric arc between the electrodes 8/9, brought together and fused with one another. During this process, the LID system 6/7 continuously measures the light transmission via the splice point. If the intensity measured in the optical receiver 7 reaches a maximum, the optimum welding period is reached and the welding operation is automatically terminated. By applying this technique, referred to as automatic fusion time control, it is possible largely to compensate the effects caused by the state of the electrodes 8/9 (non-optimum spacing, wear, etc) and/or by environmental influences (moisture, air pressure, temperature), and which lead to a rise in splice loss.

Despite every care taken and the precision exercised during the preparation, alignment and bringing together of the glass fibers 1/2, as a rule it is not possible to, ~~as a rule,~~ completely to avoid a residual offset of the fiber cores C1/C2, oblique positioning of the fiber longitudinal axes and/or of the fiber end faces, as well as an overtravel (the incipiently fused fiber ends are brought together and pushed into one another beyond the permissible extent). Depending on the extent/magnitude of these "faulty positions", it follows that in the region of the splice produced the geometry of the fiber core C1/C2 deviates more or less strongly from that of the undisturbed fiber. Since it is essentially only the fiber core that transports the light, disturbances in the core geometry in the region of the splice are chiefly responsible for the increase in the loss. Thus, methods for determining the quality of a splice can therefore supply results of high precision only when the core geometry, that is to say the spatial distribution of the refractive index $n(\vec{r})$ determining the loss response, at the splice point features in the calculation of the loss.

In the ~~case of the proposed~~ method of the invention, the splice geometry is detected in three dimensions by means of the optical systems 11 - 17 present in the splicer and therefrom the spatial distribution $n(\vec{r})$ of the refractive index that exactly describes the splice and its properties (that is to say also the loss) is derived. In

Version with Markings to Show Changes Made

detail, the determination of the splice loss requires the execution of the following steps, explained below in more detail:

- determining the splice geometry in three dimensions and calculating the spatial distribution $n(\vec{r})$ of the refractive index;
- ascertaining the field distribution ("initial field distribution" $\vec{E}(z_0)$) of a mode that can be propagated in the glass fiber (corresponding, for example, to the fundamental mode LP_{01} in what is termed a monomode glass fiber) inside a spatial region situated upstream/downstream of the splice in the beam direction;
- calculating the field distribution ("final field distribution" $\vec{E}(z_n)$) of this mode inside a spatial region situated downstream of the splice in the beam direction, and
- calculating the loss in the splice from the intensity values assigned to the two field distributions.

Detecting the splice geometry in three dimensions

Referring now to Fig. 3, a~~A~~ glass fiber serving to transport electromagnetic radiation and denoted in figure 3 by 20 consists, for example, of a Ge-doped SiO_2 core 21 ($n_{core} = 1.48$), and SiO_2 cladding 22 ($n_{cladding} = 1.46$) concentrically sheathing the core 21, and of a plastic coating 23 that protects a core 21 and cladding 22 against external mechanical, thermal and chemical actions and is usually of colored finish and, if appropriate, also provided with a ring marking. In the case of a monomode glass fiber 20, the core glass diameter is typically $\phi_{core} = 9$ µm, while the cladding glass diameter is typically $\phi_{cladding} = 125$ µm.

Since the concentration of the dopant in the glass fiber 20 has a constant value on the fiber longitudinal axis OA, and exhibits in the plane orthogonal thereto, for example, the profile illustrated in the right-hand part of Fig. ~~figure~~ 3, the spatial distribution of the refractive index $n(\vec{r})$ is also radially symmetrical with reference to the fiber longitudinal axis OA ($n(\vec{r}) = n(r,z=z_0)$). Because of the already mentioned effects (offset of the fiber core, oblique position of the fiber end faces, etc before the splicing), the spatial distribution of the refractive index $n(\vec{r})$ in the region of the splice can differ substantially in some circumstances from the refractive index distribution $n_0(\vec{r})$ of the undisturbed glass fiber. As already explained, it is essentially only the deformation of the optically conducting regions, that is to say the fiber core 21, that is responsible for the loss in intensity at the splice point. Consequently, to calculate the loss it suffices to know the spatial

Version with Markings to Show Changes Made

distribution $n(\vec{r})$ of the refractive index inside a volume containing the core 21 and extending, for example, only 20 - 40 µm in the transverse direction (x/y-plane).

Recording images of the splice

Fig. ~~ure~~ 4 shows the intensity distribution generated by the imaging optical system 14 on the sensor surface 17', defining the x/z-plane, of the CCD camera 17, when a glass fiber 20 stripped of its protective coating 22 is trans-illuminated by activating the light source 12 in the transverse direction (x-direction). Clearly in evidence are the outer contours 22' (outer edge of the fiber cladding 22) of the glass fiber 20, the two dark zones 24/24' caused by the cylinder lens effect, and the image of the fiber core 21 (pair of lines 21'). A corresponding shadow image is produced by the system, comprising the light source 11 and the imaging optical system 13, on the sensor surface, defining the x/z-plane, of the CCD camera 16. The two intensity distributions are fed via the video evaluating unit 15 to the controller 19, which is equipped with a powerful microprocessor, and stored there in digital form.

Direct calculation of distribution $n(\vec{r})$ of the refractive index from the image of the splice

If the optical systems of the splicer have a sufficiently high resolution, the spatial distribution of the refractive index $n(\vec{r})$ can be calculated directly from the recorded images, for example with the aid of the method described by D. Marcuse, "Principles of optical fiber measurement", Academic Press, 1981 [ISBN 0-12-470980-X], pages 150-165~~in [3]~~. This does not require any additional information, and the distribution of the refractive index has not to be standardized in some way. There are, however, the disadvantages of the necessary imaging optical system, which meets high demands and is ~~therefore~~therefore, comparatively expensive, and of the expenditure, additionally required in the case of some methods, for generating interference images.

Deriving the distribution of the refractive index $n(\vec{r})$ from a basic distribution $n_0(\vec{r})$

In order to determine the spatial distribution of the refractive index $n(\vec{r})$ in the region of the splice, what is termed a basic distribution $n_0(\vec{r})$ of the refractive index is modified by means of suitable parameters obtained from the recorded

Version with Markings to Show Changes Made

images of the splice. The spatial distribution of the refractive index in the undisturbed glass fiber serves, in particular, as basic distribution $n_0(\vec{r})$. Said undisturbed glass fiber is known in the case of use of specific types of glass fibers (standard fiber, dispersion-shifted fiber, erbium-doped fiber, etc), or it can be taken from the data sheet or supplied by the manufacturer upon request. If appropriate information is not available, the distribution $n_0(\vec{r})$ of the refractive index of the undisturbed fiber can be determined experimentally, for example by means of the method described by H.-G. Unger, "Optische Nachrichtentechnik", Hüthig, 1998 [ISBN 3-7785-22261-2], pages 648-671~~in~~ [4].

It is advantageous in practice for the spatial distribution, serving as basic distribution $n_0(\vec{r})$, of the refractive index of the undisturbed fiber to be determined in advance for the different, frequently used fiber types and to be stored in the splicer, if appropriate in parametric form. Since the glass fibers used in telecommunication are for the most part designed to be homogeneous in the direction of their longitudinal axis OA and to be rotationally symmetrical with reference to this axis OA, the distribution of the refractive index also has a corresponding symmetry, that is to say what is termed the refractive index profile $n(r, z_0)$ (r: lateral distance from the fiber longitudinal axis OA) describes the distribution of the refractive index completely.

The following examples explain the steps required to determine the distribution $n(\vec{r})$, featuring in the calculation of the loss, in the region of the splice by modifying a basic distribution $n_0(r)$. For the sake of clarity, the effects and mechanisms which act to increase loss and occur in practice simultaneously for the most part, are illustrated separately. The distribution $n_{\lambda 1}(\vec{r})$, determined for a wavelength $\lambda 1$, of the refractive index can be converted in this case with the aid of what is termed the Sellmaier series (for example, see Electronic Letters, Vol. 14, No. 11, May 1978, pages 326-328 [5]~~, for example~~) into the corresponding distribution $n_{\lambda 2}(\vec{r})$ in the case of another wavelength $\lambda 2$.

Offset of the fiber cores

In the ideal state, the core and cladding of the two interconnected glass fibers have the same axes of symmetry, which coincide with the z-axis, in the region of the splice, as well. However, because of incorrect positioning of at least one of the two glass fibers in advance of fusing (null alignment), offsetting of the cores which disturbs the light propagation and increases the loss occurs in the

Version with Markings to Show Changes Made

region of the splice point 25 (see Fig. ~~figure~~ 5). Consequently, in the intensity distributions produced by the imaging optical systems 13/14 on the sensor surfaces of the CCD cameras 16/17, respectively, of the splice point there is to be observed a lateral displacement, proportional to the offset, of the pairs of lines 21'/21", representing the respective cores, with reference to the z-axis, the curve describing the lateral distance x_m/y_m of the core centers from the z-axis showing the stepped profile illustrated schematically in the right-hand upper part of Fig. ~~figure~~ 5.

If the spatial distribution $n_0(\vec{r})$ of the refractive index of the undisturbed glass fiber (basic distribution) in a transverse direction has, for example, a stepped profile illustrated in the lower part of Fig. ~~figure~~ 4, the refractive index distribution $n(\vec{r})$ being sought, which approximates the real conditions, is calculated by modifying the basic distribution $n_0(\vec{r})$ in accordance with Equation (1).

$$n(r,z) = n_0(r' + \Delta r, z) \qquad (1)$$

wherein

$\Delta r^2 = x_m^2(z) + y_m^2(z)$

x_m^2 is the ——lateral displacement of the core center in the x/z-plane, and

y_m^2 is the ——lateral displacement of the core center in the y/z-plane

The refractive index profile therefore changes on the z-axis in accordance with the right-hand lower part of Fig. ~~figure~~ 5.

The offset of the pair of lines 21'/21" representing the fiber core 21 with reference to a reference position situated preferably at the left-hand or right-hand edge of the image is measured in order to extract with high accuracy from the images the lateral distances $x_m(z)/y_m(z)$ of the fiber center from the z-axis illustrated in the shadow image. The correlation method described by W. Lieber, "Verfahren zur Ausrichtung zweiter Lichtwellenleiter-Faserenden und Einrichtung zur Durchführung des Verfahrens" [Method for aligning two optical waveguide fiber ends and device for carrying out the method.], EP Application No. 90109388, 17.05.1990, ~~in [6],~~ for example, can be applied for this purpose.

If the optical system of the splicer does not permit images/visualization of the fiber core 21, it can be assumed in a first approximation that the core 21 does not significantly change its position relative to the outer contour of the fiber during fusing. The lateral distance of the middle of the core from the z-axis illustrated in

Version with Markings to Show Changes Made

the shadow image then approximately corresponds to the lateral distance of the center of the fiber outer contour 22' from this axis.

Bending of the fiber core

Bending of the fiber core in the region of the splice comes about, for example, because of the eccentric position of at least one of the two cores inside the respective glass fiber and/or the nonparallelism of the mutually opposite fiber end faces in advance of fusing. The two imaging optical systems 13/14 of the splicer then respectively generate a shadow image of the splice which is illustrated schematically in the left-hand part of Fig. ~~figure~~ 6. Outside the heating zone 26, the center of the fiber core is to be situated below on the z-axis, but to be offset in the middle 25 of the splice by $\Delta x(z_s)$ or $\Delta y(z_s)$ in the lateral direction. The lateral distance $\Delta x(z)/\Delta y(z)$ of the core center therefore changes on the z-axis in accordance with the function that is illustrated in the right-hand upper part of Fig. ~~figure~~ 6 and passes through a minimum in the middle 25 of the splice (coordinate z_s).

In order to obtain the spatial distribution, approximated to the real conditions, of the refractive index in the region of the splice, the basic distribution $n_0(r)$ is displaced in the lateral direction in accordance with the measured lateral distance $\Delta x(z)/\Delta y(z)$ of the core center from the z-axis. The right-hand lower part of figure 6 shows the profiles n(r,z) of the refractive index that are assigned to the various z-values.

Change in the cross section of the fiber core

If the two glass fibers to be connected are compressed or drawn apart from one another during the splicing operation, this produces an expansion or tapering of the fiber core and the outer contour in the region of the splice, something which influences the loss. In the shadow image of the splice that is produced (see Fig. ~~figure~~ 7), the lines 21' which delimit the fiber core from the fiber cladding and run outside the splice point approximately parallel to the z-axis then exhibit a distance from one another which is increased/reduced by comparison with the undisturbed regions situated at the edge of the image. The right-hand upper part of Fig. ~~figure~~ 7 shows the functional dependence of the widening $\Delta d_{x/y}$ of the core diameter along the z-axis. The width $d_{x/y}(z_s)$ of the core is greatest in the middle 25 of the splice. The ratio $V_{x/y}(z)$ given by Equation 2

Version with Markings to Show Changes Made

$$V_{x/y}(z) := [d_{x/y}(z)]/[d_{x/y}(z_0)] \qquad (2)$$

$d_{x/y}(z)$, the spacing of the pair of lines 21' at a point z in the region of the splice, and

$d_{x/y}(z_0)$, the spacing of the pair of lines 21' at a point z_0 outside the heating zone,

therefore defines a measure of the change in cross section of the fiber core.

In order to obtain the distribution of the refractive index at the splice point, the basic distribution $n_0(r)$ is compressed or stretched in accordance with the ratio $V_{x/y}(z)$ in the x/y-plane, such that, for example, the refractive index profile illustrated schematically in the right-hand lower part of Fig. ~~figure~~ 7 is obtained at different points on the z-axis.

If no high quality imaging system is available (core not visible in the shadow image), the change in cross section of the fiber core can be equated at least approximately to the change in cross section of the outer contour (not illustrated in Fig. ~~figure~~ 7). It therefore suffices to measure the fiber outer contours 22' in the respective shadow image, in order to determine the compression or expansion factor $V_{x/y}(z)$ that can be applied to the basic distribution.

Diffusion of the dopant in the region of the splice

During the heating of the glass fibers in the arc, the dopant responsible for the different refractive indices of core and cladding begin to migrate in the direction prescribed by the gradient of the concentration, that is to say chiefly in the lateral direction outward into the cladding. This process leads to a change in the refractive index profile that influences the loss.

Since the concentration of the dopant at the core/cladding boundary decreases as a consequence of the diffusion, the image contrast is reduced at the splice point, that is to say the pair of lines 21' representing the fiber core appear to be less dark in the shadow image produced, in particular in the middle 25 of the splice, than outside the heating zone 26, for example (see figure 8). The change $\Delta\rho_{x/y}$, caused by diffusion, in the dopant concentration on the z-axis thereby approximately follows the bell-shaped curve illustrated in the right-hand upper part of Fig. ~~figure~~ 8.

Version with Markings to Show Changes Made

In order to obtain the distribution of the refractive index n(r,z) at the splice, the basic distribution $n_0(r,z_0)$ is compressed or stretched in the lateral direction with the aid of a parameter $S_{x/y}(z) = f(K_{x/y}(z))$ dependent on the ratio

$$K_{x/y}(z) := H_{x/y}(z)/H_{x/y}(z_0) \qquad (3)$$

$H_{x/y}(z)$: brightness/intensity of the core boundary at a point z in the region of the splice

$H_{x/y}(z_0)$: brightness/intensity of the core boundary at a point z_0 outside the heating zone,

such that the distribution n(r) being sought exhibits the profile, illustrated in the right-hand lower part of figure 8, on the z-axis. The ratio $K_{x/y}(z)$ can also serve approximately as a parameter $S_{x/y}(z)$.

If the core is not to be discerned in the shadow images (simple optical system), it is possible to deduce the level of the diffusion and thus the stretch/compression factor by measuring the splicing temperature (for example directly or indirectly via the brightness of the heated fiber) or from the heating temperature set at the splicer.

Ascertaining the initial field distribution

The initial field distribution $\overline{E}_0(\overline{r})$ featuring in the calculation of the splice loss corresponds to the spatial dependence, derived from the basic distribution $n_0(\overline{r})$ of the refractive index for a given wavelength and the associated spatial region, of the electric field of a mode that can be propagated in the glass fiber (for example fundamental mode LP_{01} of a monomode glass fiber). Methods for calculating the field distribution from a prescribed spatial distribution of the refractive index are known, for example, from Siemens Forschungs- und Entwicklungsbreicht, Vol. 4, No. 3, 1985, Pages 89-96, and Journal of Lightwave Technology, Vol. 12, No. 3, March 1995, pages 487-494 ~~[7, 8]~~.

Calculating the final field distribution

The initial field distribution $\overline{E}_0(\overline{r})$, assigned to the mode that can be propagated, in a first spatial region enclosing the fiber core and situated upstream

Version with Markings to Show Changes Made

of the splice is used to calculate the spatial dependence, termed the final field distribution $\overline{E}_n(\overline{r})$ below, of the electric field of the mode, propagating from the first spatial region via the splice, within a second spatial region situated downstream of the splice in the direction of propagation, by means of one of the beam propagation methods (BPM) described in IEEE Photonics Technology Letters, Vol. 4, No. 2, February 1992, pages 148-151; Journal of Lightwave Technology, Vol. 10, No. 3, March 1992, pages 295-305; and IEEE Photonics Technology Letters, Vol. 5, No. 9, September 1993, Pages 1073-11076 ~~[9—11]~~.

_____The BPM firstly requires the refractive index distribution at discrete points in space, which is subdivided, for example, into cuboids of equal size. The edge length of each cuboid can be 0.5 μm, for example, in the z-direction, and 0.25 μm in the x- and y-direction, in each case (see Fig. ~~figure~~ 9), all the cuboids with the same z-coordinate forming a spatial region denoted as a layer. Each cuboid is assumed to be homogeneous with reference to the refractive index, that is to say the refractive index does not change inside the respective cuboid.

_____Since the distribution of the refractive index cannot be determined from the above described measurements with the accuracy required for the BPM, the missing data points are determined by interpolation (for example, using splines). This can even be done straight away, since the refractive index changes only very little between two points in space which are still just resolved by the imaging system.

_____If the electric field $\overline{E}_0(x, y, z_0)$ (termed $\overline{E}(z_0)$ below) describing a mode that can be propagated in the glass fiber and derived from the basic distribution $n_0(\overline{r})$ is present at the centers of the cuboid end faces of the first layer (symbolized by black points in Fig. ~~figure~~ 9), the BPM uses this initial field distribution and the refractive indices of the first layer to calculate the electric field $\overline{E}(x, y, z_0 + \Delta z)$ between the first and second layers and again, therefrom, the electric field $\overline{E}(x, y, z_0 + 2\Delta z)$ between the second and third layers. If the method is continued iteratively, the BPM finally supplies the electric field $\overline{E}_n(x, y, z_0 + n\Delta z)$ (termed $\overline{E}(z_n)$ below), representing the final field distribution, at the end surface of the last layer.

_____Numerous variants of the BPM exist, the desired accuracy, the required computational outlay and the tolerable computer time determining the selection of

Version with Markings to Show Changes Made

the method to be applied. Thus, the computational outlay and therefore the computer time can be reduced for a given computer power

- by using a method operating with the aid of a slowly varying envelope approximation (splice geometry deviates only negligibly from that of the undisturbed fiber),
- by applying a scalar BPM (weak transverse mode coupling), or
- by reducing the three-dimensional distribution of the refractive index, for example with the aid of the method of the effective index, to a two-dimensional problem (simple splice geometry).

Calculating the splice loss

The splice loss can be calculated from the initial field distribution $\overline{E}(z_0)$ of the final distribution $\overline{E}(z_n)$ or the corresponding intensities $I(z_0)$ and $I(z_n)$, respectively, by means of

$$L_{[dB]} = 10\log_{10}\left(\frac{I(z_0)}{I(z_n)}\right) \qquad (4)$$

The above formula assumes that $E(z_n)$ describes a mode that propagates even over relatively large distances in the fiber. If the final field distribution $\overline{E}(z_n)$ also includes amounts of modes that cannot propagate, it is necessary at first to decompose $\overline{E}(z_n)$ in accordance with the equation (4), v denoting the order of the highest mode that can still propagate, and w denoting the order of the highest mode contained in $\overline{E}(z_n)$.

$$\overline{E}(z_n) = \sum_{i=0}^{v} \overline{E}_i(z_n) + \sum_{j=v+1}^{w} \overline{E}_j(z_n) \qquad (5)$$

Consequently, the variable $\Sigma\,\overline{E}_i(z_n)$ represents the total field distribution of the modes that can propagate, and $\Sigma\,\overline{E}_j(z_n)$ represents the total field distribution of the modes that cannot propagate, the intensity $I(z_n)$ derived only from $\Sigma\,\overline{E}_i(z_n)$ featuring in the calculation of the loss.

The determination of the final field distribution from the initial field distribution requires a high computational outlay, and so it is possible, depending on the performance of the processor built into the splicer, for a relatively long time

Version with Markings to Show Changes Made

to elapse before the splice loss is indicated on the display screen. This can be avoided by no longer calculating the final field distribution directly in the splicer, but doing so in advance at the manufacturers. There, the parameters relevant to the loss are determined from a large number of recorded splice geometries and the loss values calculated using a powerful processor. These parameters need not necessarily have a physical analogy (for example core offset, etc). Methods for determining such parameters are known from statistics or physics by the designation of main components or factor analysis or Karhunen-Loeve decomposition. The functional relationship of the parameters with the calculated loss defines a characteristic diagram which is stored in each splicer. The function of the splicer then reduces to using the parameters to classify the splice produced and reading of the assigned loss from the characteristic diagram.

~~6. Literature~~

~~[1] ICCS and Future Link; catalog 1998; Siemens Communication Cable Networks; pages 107 - 116~~

~~[2] EP 0 326 988 B1~~

~~[3] D. Marcuse "Principles of optical fiber measurements", Acad. Pr., 1981, ISBN 0-12-470980-X, pages 150 - 165~~

~~[4] H. G. Unger, "Optische Nachrichtentechnik", Hüthig, 1993, ISBN 3-7785-2261-2, pages 648 - 671~~

~~[5] Electronic Letters, Vol. 14, No. 11, May 1978; pages 326 - 328~~

~~[6] W. Lieber, Th. Eder "Verfahren zur Ausrichtung zweier Lichtwellenleiter Faserenden und Einrichtung zur Durchführung des Verfahrens" ["Method for aligning two optical waveguide fiber ends and device for carrying out the method"], EP-Appl. 90109388.0, 17.05.1990~~

~~[7] Siemens Forschungs- und Entwicklungsbericht, Volume 14, No. 3, 1985; pages 89 - 96~~

~~[8] Journal of Lightwave Technology, Vol. 12, No. 3; pages 487 - 494, March 1994~~

~~[9] IEEE Photonics Technology Letters, Vol. 4, No. 2, pages 148 - 151, February 1992~~

~~[10] Journal of Lightwave Technology, Vol. 10, No. 3; pages 295 - 305, March 1992~~

~~[11] IEEE Photonics Technology Letters, Vol. 5, No. 9; pages 1073 - 1076, September 1993~~

Version with Markings to Show Changes Made

~~Patent claims~~

~~1. A method for determining the loss of a splice connecting two optical waveguides by executing the following steps:~~

~~a) determining or describing a first spatial distribution of the refractive index ($n_0(\vec{r})$) inside a first spatial region, not influenced by the splice, of a first optical waveguide,~~

~~b) determining a second spatial distribution ($n(\vec{r})$) of the refractive index in the region of the splice,~~

~~c) deriving a first field function ($\vec{E}(z_0)$) from the first spatial distribution ($n_0(\vec{r})$) of the refractive index, the first field function ($\vec{E}(z_0)$) describing the spatial dependence of the electric field of a mode that can propagate in the waveguides,~~

~~d) calculating a second field function ($\vec{E}(z_n)$) from the first field function ($\vec{E}(z_0)$) and the second spatial distribution of the refractive index ($n(\vec{r})$), the second field function ($\vec{E}(z_n)$) describing the spatial dependence of the electric field, the mode propagating from the first spatial region via the splice, within a second spatial region, not influenced by the splice, of the second optical waveguide,~~

~~e) calculating a first intensity ($I(z_0)$) and a second intensity ($I(z_n)$) from the assigned field functions ($\vec{E}(z_0)$, $\vec{E}(z_n)$), and~~

~~f) calculating the loss (L) of the splice occurring as a function of the ratio of the two intensities ($I(z_0)$, $I(z_n)$).~~

~~2. The method as claimed in claim 1, characterized in that the loss (L) of the splice is calculated in accordance with the relationship~~

$$L_{[dB]} = 10\log_{10}\left(\frac{I(z_0)}{I(z_n)}\right)$$

Version with Markings to Show Changes Made

~~3. The method as claimed in claim 1 or 2, characterized in that the second spatial distribution ($n(\vec{r})$) of the refractive index is determined by transverse irradiation of the splice with light and evaluation of the intensity distribution generated downstream of the splice in the beam direction, or of the shadow image.~~

~~4. The method as claimed in claim 3, characterized in that the waveguides and the splice are transilluminated from two directions enclosing an angle of $\alpha \neq 180°$, and in that the transmitted radiation is projected in each case by means of an optical system (13, 14) onto a sensor or detector element (16, 17) defining a plane.~~

~~5. The method as claimed in claim 4, characterized in that the planes respectively defined by the sensor or detector element (16, 17) enclose an angle of approximately 90°.~~

~~6. The method as claimed in one of claims 3 to 5, characterized in that an offset of the center of the optically conducting core of the waveguides in the region of the splice is determined at least in a first spatial direction from the shadow image, in that the first spatial distribution of the refractive index corresponding to the offset of the light conducting core is displaced in the corresponding spatial direction, and in that the modified first spatial distribution of the refractive index represents the second spatial distribution of the refractive index.~~

~~7. The method as claimed in claim 6, characterized in that the offset of the optically conducting core is derived from the offset of the center line of the outer contour of the waveguides in the region of the splice.~~

Version with Markings to Show Changes Made

~~8. The method as claimed in one of claims 3 to 5, characterized in that a tapering or expansion of the light conducting core of the waveguides in the region of the splice is determined at least in a first spatial direction from the shadow image, in that the first spatial distribution of the refractive index is compressed or stretched in the corresponding spatial direction by a factor proportional to the ratio $[d_{x/y}(z)]/[d_{x/y}(z_0)]$, $d_{x/y}(z_0)$ denoting the width of the core at a point z_0, not influenced by the splice, of the waveguides, and $d_{x/y}(z)$ denoting the width of the core at a point z lying in the region of the splice, and in that the correspondingly compressed or elongated first spatial distribution of the refractive index represents the second spatial distribution of the refractive index.~~

~~9. The method as claimed in claim 8, characterized in that the tapering or expansion or of the light guiding core is derived respectively from the tapering or expansion of the outer contour of the waveguides in the region of the splice.~~

~~10. The method as claimed in one of claims 3 to 5, characterized in that the brightness of an edge delimiting the light guiding core of the cladding of the waveguide is of the measured in at least one of the two shadow images in the region of the splice and in a second region not influenced by the splice, in that the first spatial distribution of the refractive index is spatially modified in accordance with a factor dependent on the measured brightnesses, and in that the modified first spatial distribution of the refractive index represents the second spatial distribution of the refractive index.~~

Version with Markings to Show Changes Made

Patent Claims:

11. A method for determining the loss of a splice connecting two optical waveguides by executing the following steps:

a) determining or describing a first spatial distribution of the refractive index ($n_0(\vec{r})$) inside a first spatial region, not influenced by the splice, of a first optical waveguide,

b) determining a second spatial distribution ($n(\vec{r})$) of the refractive index in the region of the splice,

c) deriving a first field function ($\vec{E}(z_0)$) from the first spatial distribution ($n_0(\vec{r})$) of the refractive index, the first field function ($\vec{E}(z_0)$) describing the spatial dependence of the electric field of a mode that can propagate in the waveguides,

d) calculating a second field function ($\vec{E}(z_n)$) from the first field function ($\vec{E}(z_0)$) and the second spatial distribution of the refractive index ($n(\vec{r})$), the second field function ($\vec{E}(z_n)$) describing the spatial dependence of the electric field, the mode propagating from the first spatial region via the splice, within a second spatial region, not influenced by the splice, of the second optical waveguide,

e) calculating a first intensity ($I(z_0)$) and a second intensity ($I(z_n)$) from the assigned field functions ($\vec{E}(z_0)$, $\vec{E}(z_n)$), and

f) calculating the loss (L) of the splice occurring as a function of the ratio of the two intensities ($I(z_0)$, $I(z_n)$).

12. The method according to claim 11, wherein ~~as claimed in claim 11, characterized in that~~ the loss (L) of the splice is calculated in accordance with the relationship

$$L_{[dB]} = 10\log_{10}\left(\frac{I(z_0)}{I(z_n)}\right)$$

13. The method according to claim 11, wherein ~~as claimed in claim 11, characterized in that~~ the second spatial distribution ($n(\vec{r})$) of the refractive index is determined by transverse irradiation of the splice with light and evaluation of the

intensity distribution generated downstream of the splice in the beam direction, or of the shadow image.

14. The method according to claim 12, wherein ~~as claimed in claim 12, characterized in that~~ the second spatial distribution ($n(\vec{r})$) of the refractive index is determined by transverse irradiation of the splice with light and evaluation of the intensity distribution generated downstream of the splice in the beam direction, or of the shadow image.

15. The method according to claim 13, wherein ~~as claimed in claim 13, characterized in that~~ the waveguides and the splice are trans-illuminated from two directions enclosing an angle of $\alpha \neq 180°$, and in that the transmitted radiation is projected in each case by means of an optical system ~~(13, 14)~~ onto a sensor or detector element ~~(16, 17)~~ defining a plane.

16. The method according to claim 14, wherein ~~as claimed in claim 14, characterized in that~~ the waveguides and the splice are trans-illuminated from two directions enclosing an angle of $\alpha \neq 180°$, and in that the transmitted radiation is projected in each case by means of an optical system ~~(13, 14)~~ onto a sensor or detector element ~~(16, 17)~~ defining a plane.

17. The method according to claim 15, wherein ~~as claimed in claim 15, characterized in that~~ the planes respectively defined by the sensor or detector element ~~(16, 17)~~ enclose an angle of approximately 90°.

18. The method according to claim 16, wherein ~~as claimed in claim 16, characterized in that~~ the planes respectively defined by the sensor or detector element ~~(16, 17)~~ enclose an angle of approximately 90°.

19. The method according to claim 13, wherein ~~as claimed in one of claims 13, characterized in that~~ an offset of the center of the optically-conducting core of the

Version with Markings to Show Changes Made

waveguides in the region of the splice is determined at least in a first spatial direction from the shadow image, in that the first spatial distribution of the refractive index corresponding to the offset of the light-conducting core is displaced in the corresponding spatial direction, and ~~in that~~ the modified first spatial distribution of the refractive index represents the second spatial distribution of the refractive index.

20. The method ~~as claimed in one of claims 14, characterized in that~~ according to claim 14, wherein an offset of the center of the optically-conducting core of the waveguides in the region of the splice is determined at least in a first spatial direction from the shadow image, in that the first spatial distribution of the refractive index corresponding to the offset of the light-conducting core is displaced in the corresponding spatial direction, and in that the modified first spatial distribution of the refractive index represents the second spatial distribution of the refractive index.

21. The method according to claim 19, wherein ~~as claimed in claim 19, characterized in that~~ the offset of the optically-conducting core is derived from the offset of the center line of the outer contour of the waveguides in the region of the splice.

22. The method according to claim 20, wherein ~~as claimed in claim 20, characterized in that~~ the offset of the optically-conducting core is derived from the offset of the center line of the outer contour of the waveguides in the region of the splice.

23. The method according to claim 13, wherein ~~as claimed in one of claims 13, characterized in that~~ a tapering or expansion of the light-conducting core of the waveguides in the region of the splice is determined at least in a first spatial direction from the shadow image, in that the first spatial distribution of the refractive index is compressed or stretched in the corresponding spatial direction by a factor proportional to the ratio $[d_{x/y}(z)]/[d_{x/y}(z_0)]$, $d_{x/y}(z_0)$ denoting the width of the core at a point z_0, not influenced by the splice, of the waveguides, and $d_{x/y}(z)$ denoting the width of the core at a point z lying in the region of the splice, and in that the correspondingly compressed or

elongated first spatial distribution of the refractive index represents the second spatial distribution of the refractive index.

24. The method according to claim 14, wherein ~~as claimed in one of claims 14, characterized in that~~ a tapering or expansion of the light-conducting core of the waveguides in the region of the splice is determined at least in a first spatial direction from the shadow image, in that the first spatial distribution of the refractive index is compressed or stretched in the corresponding spatial direction by a factor proportional to the ratio $[d_{x/y}(z)]/[d_{x/y}(z_0)]$, $d_{x/y}(z_0)$ denoting the width of the core at a point z_0, not influenced by the splice, of the waveguides, and $d_{x/y}(z)$ denoting the width of the core at a point z lying in the region of the splice, and in that the correspondingly compressed or elongated first spatial distribution of the refractive index represents the second spatial distribution of the refractive index.

25. The method according to claim 23, wherein ~~as claimed in claim 23, characterized in that~~ the tapering or expansion or of the light-guiding core is derived respectively from the tapering or expansion of the outer contour of the waveguides in the region of the splice.

26. The method acording to claim 24, wherein ~~as claimed in claim 24, characterized in that~~ the tapering or expansion or of the light-guiding core is derived respectively from the tapering or expansion of the outer contour of the waveguides in the region of the splice.

27. The method according to claim 13, wherein ~~as claimed in one of claims 13, characterized in that~~ the brightness of an edge delimiting the light-guiding core of the cladding of the waveguide is of the measured in at least one of the two shadow images in the region of the splice and in a second region not influenced by the splice, in that the first spatial distribution of the refractive index is spatially modified in accordance with a factor dependent on the measured brightnesses, and in that the modified first spatial

Version with Markings to Show Changes Made

distribution of the refractive index represents the second spatial distribution of the refractive index.

28. The method according to claim 14, wherein ~~as claimed in one of claims 14, characterized in that~~ the brightness of an edge delimiting the light-guiding core of the cladding of the waveguide is of the measured in at least one of the two shadow images in the region of the splice and in a second region not influenced by the splice, in that the first spatial distribution of the refractive index is spatially modified in accordance with a factor dependent on the measured brightnesses, and in that the modified first spatial distribution of the refractive index represents the second spatial distribution of the refractive index.

Version with Markings to Show Changes Made

Abstract Of The Invention

The invention relates to methods for determining the attenuation of a splice connecting two optical waveguides. Methods for assessing the quality of the splice provide high precision results only when the dimensions of the light-conducting fiber, i.e., the spatial distribution of the refractive index which determines the attenuation behavior, are used in the calculation of the attenuation. The dimensions of the splice are measured in a three-dimensional manner by optical systems, and the spatial distribution of the refractive index of the splice is derived therefrom. The field distribution corresponding to a mode that is capable of propagating in the fiber is fixed within a first spatial region situated in front of the splice in the beam direction; and the field distribution of this mode is determined within a second spatial region situated behind the splice in a beam direction while taking into consideration the spatial distribution of the refractive index of the splice. The splice attenuation is calculated from the intensity values assigned to both field distributions

Clean Version of Amended Application

SI01-030

CALCULATING SPLICE LOSS BY GEOMETRIC MEASUREMENT

Cross-Reference To Related Applications

[0001] This application claims the benefit of priority under 35 U.S.C. § 119 of German Patent Application No. 19927583.1 filed June 16, 1999, and is a national stage filing under 35 U.S.C. § 371 of PCT Application PCT/DE00/02008, filed June 16, 2000.

Field of the Invention

[0002] The invention is directed to optical waveguides, and in particular to methods for determining the attenuation of a splice connecting two optical waveguides. The splice attenuation is calculated from the intensity values assigned to field distributions, before and after the splice, corresponding to a mode that is capable of propagating in the fiber.

Background of the Invention

[0003] The method known as "thermal splicing" can be used to interconnect both monomode and multimode glass fibers and glass fiber strips in a bonded, low-loss and permanent fashion. Since the costs of constructing an optical waveguide cable network are not inconsiderably influenced by splicing as a work step that is frequently to be carried out, convenient devices which can also be used on site under difficult conditions have been developed which execute all the steps required for welding glass fibers in a largely fully automatic fashion (see ICCS and Future-Link; catalog 1998; Siemens-Communication-Cable Networks; pages 107 - 116). The loss in the splice junction produced in such a device is a function, inter alia, of the exact alignment of the optically conducting fiber cores, the quality of the fiber end faces (roughness, angle of fracture, etc) and of the welding parameters (welding time, welding current) selected by the operator or described by the respective control program.

[0004] Disturbances in the geometry of the optically conducting fiber core are decisive for the magnitude of the loss in the splice produced. In particular, the loss caused by a core offset, bending of the core or widening or tapering of the core can be determined, for example, by means of a transmission measurement and the use of a bending coupler (LID system) installed in the splicer. In this case, light is coupled into the glass fiber upstream of the splice point, and coupled out again downstream of the splice point. The intensity of the light transmitted from one glass fiber into the other glass fiber via the splice is then a measure of the loss. This measurement method cannot be applied, however, when an excessively thick or dark-colored fiber coating prevents light from being coupled into and out of the fiber core.

[0005] The method disclosed in EP 0 326 988 B1 for determining the splice loss is based on the optical detection of the core offset, the oblique position of the fiber cores and the core bending in the region of the splice point. An empirically determined formula describes the functional dependence of the loss on the said parameters. Since the method does not require light to be coupled into and out of the fiber core, it can always be applied independently of the light-passing capability of the fiber coating. However, it supplies reliable loss values only when the previously named parameters alone determine the loss of the splice. However, this is not always the case, particularly with wrongly set welding parameters or high losses.

Summary of The Invention

[0006] The invention is directed to a method for determining the loss in a splice connecting two optical waveguides. The term "splice" in this case denotes that bonded connection, in particular produced by thermal fusing/welding, between at least two optically conducting structures or elements, that is to say, in particular, the connection between glass fibers, glass fiber strips/ glass fiber bundles or the connection between a glass fiber or a glass fiber strip and an active or passive optical component.

Brief Description Of The Drawings

[0007] The invention is explained in more detail below with the aid of drawings, in which:

[0008] Fig. 1 shows the schematic structure of a modern thermal splicer operating largely fully automatically.

[0009] Fig. 2 illustrates the relative position of the ends of two optical fibers that are to be connected:

a) after being brought together and coarsely positioned;
b) after being aligned with reference to their outer contours, and
c) after being aligned with reference to their optically conducting fiber cores;

[0010] Fig. 3 shows the schematic structure of a glass fiber, and the profile n(r) of the refractive index in the plane oriented perpendicular to the fiber longitudinal axis.

[0011] Fig. 4 illustrates the intensity distribution ("shadow image" of the glass fiber) produced in the case of transverse transillumination of a glass fiber, by means of an imaging optical system in the sensor plane of a CCD camera.

[0012] Fig. 5 illustrates the shadow image of the glass fiber whose core has a lateral offset in the region of the splice.

[0013] Fig. 6 illustrates the shadow image of a glass fiber whose core is bent in the region of the splice.

[0014] Fig. 7 illustrates the shadow image of a glass fiber whose core is expanded/compressed in the region of the splice.

[0015] Fig. 8 illustrates the shadow image of a glass fiber in the case of which, because of the diffusion of the dopant atoms, the pair of lines defining the core exhibit a lesser brightness or a lesser contrast in the region of the splice than outside the heating zone.

[0016] Fig. 9 illustrates the subdivision into cuboids and layers of the space on which the method of field calculation is based and containing the fiber core.

Detailed Description of The Invention

[0017] The method is intended to enable the user to determine the loss in the splice produced, doing so with high accuracy while taking account of all the parameters substantially influencing the loss. This object is achieved by means of a method having the features specified in patent claim 1. The dependent claims relate to advantageous embodiments and developments of the method.

[0018] The proposed method can be applied straight away in a modern splicer, since all that is needed is to adapt its software appropriately. The method is distinguished, furthermore, by the following properties:

- the achievable accuracy of the determination of loss is limited essentially only by the quality of the optical system serving to visualize the fiber core and the performance of the processor executing the field calculation;
- the loss in the splice can be determined as a function of direction;
- comparatively thick and/or darkly colored fiber coatings cannot impair the measurement;
- the splice loss can be calculated for any desired operating wavelength, and
- the method permits simple adaptation to the respective requirements (for example high accuracy, fast measurement).

[0019] The splicer illustrated only schematically in Fig. 1 permits optical fibers to be welded in a largely fully automatic fashion. The bonded connection of the optical fibers that is produced with the aid of an arc (electric glow discharge) struck between two electrodes, which is denoted below as "splice" for short, is free of inclusions, the loss caused by the splice being on average approximately L = 0.02 -0.03 dB (identical standard monomode glass fibers).

[0020] The connection of the monomode or multimode glass fibers consisting in each case of a core (refractive index n_{core}), a cladding (refractive index $n_{cladding} < n_{core}$) and a coating of one or more layers is usually performed by executing the following method steps:

a) preparing the fiber ends 1/2, that is to say carefully removing the fiber coating, cleaning the fiber ends 1/2 and breaking the fibers in such a way that the fiber end faces are orientated approximately perpendicular to the fiber longitudinal axis (angle of fracture < 0.8°; typically 0.5°);

b) fixing the fiber ends 1/2 in the holders of the splicer;

c) bringing the fiber ends 1/2 together and aligning them by means of high-precision positioning units 3/4/5 by using the LID system 6/7 (Local Injection and Detection) and/or by video image evaluation;

d) cleaning the fiber end faces by briefly heating the fiber ends 1/2;

e) feeding the fiber ends 1/2 and fusing them by striking an electric arc between two electrodes 8/9 arranged in the region of the fiber ends 1/2, and

f) checking the quality of the splice (measuring the splice loss, checking the tensile strength).

[0021] Whereas the method steps a) and b) must be executed by the operator, that is to say still have to be done manually, the method steps specified under c) to f) and mentioned further in Catalog 1998 cited above, in particular the determination of the angle of fracture, the quality and the level of contamination of the fiber end faces run under program control in the splicer.

[0022] Referring now to Fig. 1, the splicer is equipped with the following components and elements in order to carry out these method steps:

- three positioning units 3, 4, and 5 for independently displacing the fiber ends 1/2, respectively guided in V grooves, in three orthogonal spatial directions (x-, y- and z-axis ≅ fiber longitudinal axis),
- a control unit 10 for driving the actuating elements (positioning motors, piezoelectric actuators) of the positioning units 3, 4 and 5,
- a transmission measuring device consisting of an optical transmitter 6 (light-emitting diode, bending coupler) and an optical receiver 7 (bending coupler, photodiode, amplifier) (LID system, see Catalog 1998 cited above),
- two optical systems for projecting the outer contours or the profile of the two fiber ends 1/2 into two planes (x/z- or y/z-plane) orientated orthogonally relative to one another, the optical systems respectively have a light source 11/12 (light-emitting diode), an imaging optical system 13/14 and a CCD camera 16/17 which is connected to the video evaluating unit 15 and defines the x/z or the y/z sensor plane,
- a heat source for heating the fiber ends 1/2 to the melting temperature, situated in the region between approximately 1600-2000°C, the supply of heat being performed in the

exemplary embodiment shown by means of a glow discharge produced between two electrodes 8/9 and controlled by the unit 18,

- a central controller 19 which is connected on the input side to the video evaluating unit 15 and executes and monitors all the steps required for splicing in accordance with the selected program, and
- an LCD monitor (not illustrated).

[0023] After the glass fibers have been inserted into the holder of the splicer, their ends 1/2 are not generally aligned opposite one another. As illustrated in Fig. 2 schematically in side view, both the outer contours of the fiber ends 1/2 and the fiber cores C1/C2 then do not necessarily exhibit a transverse offset δ_k or δ_c of the same size. The offset δ_k of the outer contours is now measured by evaluating the projections, recorded with the aid of the two CCD cameras 16/17, of the fiber ends 1/2 in the x/z-plane or the y/z-plane. Subsequently, the fiber ends 1/2 are displaced with the aid of the first positioning units 3, 4 and 5 , driven with the aid of the control unit 10, in a transverse direction, that is to say in the direction of the x- and y-axes until the outer contours of the fiber ends 1/2 are aligned, their transverse offset δ_k thus vanishing at least approximately ($\delta_{kx} \approx \delta_{ky} \approx 0$) both in the x- and in the y-directions. After this alignment, referred to as fine positioning, the fiber ends 1/2 are situated opposite one another, as illustrated in Fig. 2b. The core offset δ_c, caused by the eccentric position of the fiber cores C1/C2, which is still present is clearly to be seen.

[0024] In order to produce a splice with the lowest possible loss, the fiber ends 1/2 must therefore further be aligned with regard to their cores C1/C2, that is to say the core offset δ_c must be removed or at least minimized. This is performed by using the LID system, which feeds the IR radiation, emitted by a light-emitting diode on the transmitter 6, of wavelength 800 nm $\leq \lambda \leq$ 1600 nm, in particular λ = 1300 nm or λ = 1550 nm, into the left-hand glass fiber via the assigned bending coupler, and measures the intensity of the radiation, coupled from the left-hand fiber end 1 into the right-hand fiber end 2, by means of the optical receiver, consisting of a second bending coupler and a photodiode amplifier unit. The fiber ends 1/2 are displaced in this case in the transverse direction until the radiation intensity measured in the optical receiver 7 of the LID system reaches a maximum, the fiber ends 1/2 thereby assuming the position illustrated in Fig. 2c (fiber cores C1/C2 in line and aligned in parallel with the z-axis; small contour offset corresponding to the corrected core offset δ_c).

[0025] Subsequently, the fiber ends 1/2 are heated by striking the electric arc between the electrodes 8/9, brought together and fused with one another. During this process, the LID system 6/7 continuously measures the light transmission via the splice point. If the intensity measured in the optical receiver 7 reaches a maximum, the optimum welding period is

reached and the welding operation is automatically terminated. By applying this technique, referred to as automatic fusion time control, it is possible largely to compensate the effects caused by the state of the electrodes 8/9 (non-optimum spacing, wear, etc) and/or by environmental influences (moisture, air pressure, temperature), and which lead to a rise in splice loss.

[0026] Despite every care taken and the precision exercised during the preparation, alignment and bringing together of the glass fibers 1/2, as a rule it is not possible to completely to avoid a residual offset of the fiber cores C1/C2, oblique positioning of the fiber longitudinal axes and/or of the fiber end faces, as well as an overtravel (the incipiently fused fiber ends are brought together and pushed into one another beyond the permissible extent). Depending on the extent/magnitude of these "faulty positions", it follows that in the region of the splice produced the geometry of the fiber core C1/C2 deviates more or less strongly from that of the undisturbed fiber. Since it is essentially only the fiber core that transports the light, disturbances in the core geometry in the region of the splice are chiefly responsible for the increase in the loss. Thus, methods for determining the quality of a splice can therefore supply results of high precision only when the core geometry, that is to say the spatial distribution of the refractive index $n(\overline{r})$ determining the loss response, at the splice point features in the calculation of the loss.

[0027] In the method of the invention, the splice geometry is detected in three dimensions by means of the optical systems 11 - 17 present in the splicer and therefrom the spatial distribution $n(\overline{r})$ of the refractive index that exactly describes the splice and its properties (that is to say also the loss) is derived. In detail, the determination of the splice loss requires the execution of the following steps, explained below in more detail:

- determining the splice geometry in three dimensions and calculating the spatial distribution $n(\overline{r})$ of the refractive index;
- ascertaining the field distribution ("initial field distribution" $\overline{E}(z_0)$) of a mode that can be propagated in the glass fiber (corresponding, for example, to the fundamental mode LP_{01} in what is termed a monomode glass fiber) inside a spatial region situated upstream/downstream of the splice in the beam direction;
- calculating the field distribution ("final field distribution" $\overline{E}(z_n)$) of this mode inside a spatial region situated downstream of the splice in the beam direction, and
- calculating the loss in the splice from the intensity values assigned to the two field distributions.

Detecting the splice geometry in three dimensions

[0028] Referring now to Fig. 3, a glass fiber serving to transport electromagnetic radiation and denoted in figure 3 by 20 consists, for example, of a Ge-doped SiO_2 core 21 ($n_{core} = 1.48$), and SiO_2 cladding 22 ($n_{cladding} = 1.46$) concentrically sheathing the core 21, and of a plastic coating 23 that protects a core 21 and cladding 22 against external mechanical, thermal and chemical actions and is usually of colored finish and, if appropriate, also provided with a ring marking. In the case of a monomode glass fiber 20, the core glass diameter is typically $\phi_{core} = 9$ µm, while the cladding glass diameter is typically $\phi_{cladding} = 125$ µm.

[0029] Since the concentration of the dopant in the glass fiber 20 has a constant value on the fiber longitudinal axis OA, and exhibits in the plane orthogonal thereto, for example, the profile illustrated in the right-hand part of Fig. 3, the spatial distribution of the refractive index $n(\vec{r})$ is also radially symmetrical with reference to the fiber longitudinal axis OA ($n(\vec{r}) = n(r,z=z_0)$). Because of the already mentioned effects (offset of the fiber core, oblique position of the fiber end faces, etc before the splicing), the spatial distribution of the refractive index $n(\vec{r})$ in the region of the splice can differ substantially in some circumstances from the refractive index distribution $n_0(\vec{r})$ of the undisturbed glass fiber. As already explained, it is essentially only the deformation of the optically conducting regions, that is to say the fiber core 21, that is responsible for the loss in intensity at the splice point. Consequently, to calculate the loss it suffices to know the spatial distribution $n(\vec{r})$ of the refractive index inside a volume containing the core 21 and extending, for example, only 20 - 40 µm in the transverse direction (x/y-plane).

Recording images of the splice

[0030] Fig. 4 shows the intensity distribution generated by the imaging optical system 14 on the sensor surface 17', defining the x/z-plane, of the CCD camera 17, when a glass fiber 20 stripped of its protective coating 22 is trans-illuminated by activating the light source 12 in the transverse direction (x-direction). Clearly in evidence are the outer contours 22' (outer edge of the fiber cladding 22) of the glass fiber 20, the two dark zones 24/24' caused by the cylinder lens effect, and the image of the fiber core 21 (pair of lines 21'). A corresponding shadow image is produced by the system, comprising the light source 11 and the imaging optical system 13, on the sensor surface, defining the x/z-plane, of the CCD camera 16. The two intensity distributions are fed via the video evaluating unit 15 to the controller 19, which is equipped with a powerful microprocessor, and stored there in digital form.

Direct calculation of distribution $n(\vec{r})$ of the refractive index from the image of the splice

[0031] If the optical systems of the splicer have a sufficiently high resolution, the spatial distribution of the refractive index $n(\vec{r})$ can be calculated directly from the recorded images, for example with the aid of the method described by D. Marcuse, "Principles of optical fiber measurement", Academic Press, 1981 [ISBN 0-12-470980-X], pages 150-165. This does not require any additional information, and the distribution of the refractive index has not to be standardized in some way. There are, however, the disadvantages of the necessary imaging optical system, which meets high demands and is therefore, comparatively expensive, and of the expenditure, additionally required in the case of some methods, for generating interference images.

Deriving the distribution of the refractive index $n(\vec{r})$ from a basic distribution $n_0(\vec{r})$

[0032] In order to determine the spatial distribution of the refractive index $n(\vec{r})$ in the region of the splice, what is termed a basic distribution $n_0(\vec{r})$ of the refractive index is modified by means of suitable parameters obtained from the recorded images of the splice. The spatial distribution of the refractive index in the undisturbed glass fiber serves, in particular, as basic distribution $n_0(\vec{r})$. Said undisturbed glass fiber is known in the case of use of specific types of glass fibers (standard fiber, dispersion-shifted fiber, erbium-doped fiber, etc), or it can be taken from the data sheet or supplied by the manufacturer upon request. If appropriate information is not available, the distribution $n_0(\vec{r})$ of the refractive index of the undisturbed fiber can be determined experimentally, for example by means of the method described by H.-G. Unger, "Optische Nachrichtentechnik", Hüthig, 1998 [ISBN 3-7785-22261-2], pages 648-671.

[0033] It is advantageous in practice for the spatial distribution, serving as basic distribution $n_0(\vec{r})$, of the refractive index of the undisturbed fiber to be determined in advance for the different, frequently used fiber types and to be stored in the splicer, if appropriate in parametric form. Since the glass fibers used in telecommunication are for the most part designed to be homogeneous in the direction of their longitudinal axis OA and to be rotationally symmetrical with reference to this axis OA, the distribution of the refractive index also has a corresponding symmetry, that is to say what is termed the refractive index profile $n(r, z_0)$ (r: lateral distance from the fiber longitudinal axis OA) describes the distribution of the refractive index completely.

[0034] The following examples explain the steps required to determine the distribution $n(\vec{r})$, featuring in the calculation of the loss, in the region of the splice by modifying a basic distribution $n_0(r)$. For the sake of clarity, the effects and mechanisms which act to increase

loss and occur in practice simultaneously for the most part, are illustrated separately. The distribution $n_{\lambda 1}(\vec{r})$, determined for a wavelength $\lambda 1$, of the refractive index can be converted in this case with the aid of what is termed the Sellmaier series (for example, see Electronic Letters, Vol. 14, No. 11, May 1978, pages 326-328) into the corresponding distribution $n_{\lambda 2}(\vec{r})$ in the case of another wavelength $\lambda 2$.

Offset of the fiber cores

[0035] In the ideal state, the core and cladding of the two interconnected glass fibers have the same axes of symmetry, which coincide with the z-axis, in the region of the splice, as well. However, because of incorrect positioning of at least one of the two glass fibers in advance of fusing (null alignment), offsetting of the cores which disturbs the light propagation and increases the loss occurs in the region of the splice point 25 (see Fig. 5). Consequently, in the intensity distributions produced by the imaging optical systems 13/14 on the sensor surfaces of the CCD cameras 16/17, respectively, of the splice point there is to be observed a lateral displacement, proportional to the offset, of the pairs of lines 21'/21", representing the respective cores, with reference to the z-axis, the curve describing the lateral distance x_m/y_m of the core centers from the z-axis showing the stepped profile illustrated schematically in the right-hand upper part of Fig. 5.

[0036] If the spatial distribution $n_0(\vec{r})$ of the refractive index of the undisturbed glass fiber (basic distribution) in a transverse direction has, for example, a stepped profile illustrated in the lower part of Fig. 4, the refractive index distribution $n(\vec{r})$ being sought, which approximates the real conditions, is calculated by modifying the basic distribution $n_0(\vec{r})$ in accordance with Equation (1).

$$n(r,z) = n_0(r' + \Delta r, z) \qquad (1)$$

wherein

$\Delta r^2 = x_m^2(z) + y_m^2(z)$

x_m is the lateral displacement of the core center in the x/z-plane, and

y_m is the lateral displacement of the core center in the y/z-plane

The refractive index profile therefore changes on the z-axis in accordance with the right-hand lower part of Fig. 5.

[0037] The offset of the pair of lines 21'/21" representing the fiber core 21 with reference to a reference position situated preferably at the left-hand or right-hand edge of the image is

measured in order to extract with high accuracy from the images the lateral distances $x_m(z)/y_m(z)$ of the fiber center from the z-axis illustrated in the shadow image. The correlation method described by W. Lieber, "Verfahren zur Ausrichtung zweiter Lichtwellenleiter-Faserenden und Einrichtung zur Durchführung des Verfahrens" [Method for aligning two optical waveguide fiber ends and device for carrying out the method.], EP Application No. 90109388, 17.05.1990, for example, can be applied for this purpose.

[0038] If the optical system of the splicer does not permit images/visualization of the fiber core 21, it can be assumed in a first approximation that the core 21 does not significantly change its position relative to the outer contour of the fiber during fusing. The lateral distance of the middle of the core from the z-axis illustrated in the shadow image then approximately corresponds to the lateral distance of the center of the fiber outer contour 22' from this axis.

Bending of the fiber core

[0039] Bending of the fiber core in the region of the splice comes about, for example, because of the eccentric position of at least one of the two cores inside the respective glass fiber and/or the nonparallelism of the mutually opposite fiber end faces in advance of fusing. The two imaging optical systems 13/14 of the splicer then respectively generate a shadow image of the splice which is illustrated schematically in the left-hand part of Fig. 6. Outside the heating zone 26, the center of the fiber core is to be situated below on the z-axis, but to be offset in the middle 25 of the splice by $\Delta x(z_s)$ or $\Delta y(z_s)$ in the lateral direction. The lateral distance $\Delta x(z)/\Delta y(z)$ of the core center therefore changes on the z-axis in accordance with the function that is illustrated in the right-hand upper part of Fig. 6 and passes through a minimum in the middle 25 of the splice (coordinate z_s).

[0040] In order to obtain the spatial distribution, approximated to the real conditions, of the refractive index in the region of the splice, the basic distribution $n_0(r)$ is displaced in the lateral direction in accordance with the measured lateral distance $\Delta x(z)/\Delta y(z)$ of the core center from the z-axis. The right-hand lower part of figure 6 shows the profiles n(r,z) of the refractive index that are assigned to the various z-values.

Change in the cross section of the fiber core

[0041] If the two glass fibers to be connected are compressed or drawn apart from one another during the splicing operation, this produces an expansion or tapering of the fiber core and the outer contour in the region of the splice, something which influences the loss. In the

shadow image of the splice that is produced (see Fig. 7), the lines 21' which delimit the fiber core from the fiber cladding and run outside the splice point approximately parallel to the z-axis then exhibit a distance from one another which is increased/reduced by comparison with the undisturbed regions situated at the edge of the image. T he right-hand upper part of Fig. 7 shows the functional dependence of the widening $\Delta d_{x/y}$ of the core diameter along the z-axis. The width $d_{x/y}(z_s)$ of the core is greatest in the middle 25 of the splice. The ratio $V_{x/y}(z)$ given by Equation 2

$$V_{x/y}(z): = [d_{x/y}(z)]/[d_{x/y}(z_0)] \qquad (2)$$

$d_{x/y}(z)$, the spacing of the pair of lines 21' at a point z in the region of the splice, and $d_{x/y}(z_0)$, the spacing of the pair of lines 21' at a point z_0 outside the heating zone, therefore defines a measure of the change in cross section of the fiber core.

[0042] In order to obtain the distribution of the refractive index at the splice point, the basic distribution $n_0(r)$ is compressed or stretched in accordance with the ratio $V_{x/y}(z)$ in the x/y-plane, such that, for example, the refractive index profile illustrated schematically in the right-hand lower part of Fig. 7 is obtained at different points on the z-axis.

[0043] If no high quality imaging system is available (core not visible in the shadow image), the change in cross section of the fiber core can be equated at least approximately to the change in cross section of the outer contour (not illustrated in Fig. 7). It therefore suffices to measure the fiber outer contours 22' in the respective shadow image, in order to determine the compression or expansion factor $V_{x/y}(z)$ that can be applied to the basic distribution.

Diffusion of the dopant in the region of the splice

[0044] During the heating of the glass fibers in the arc, the dopant responsible for the different refractive indices of core and cladding begin to migrate in the direction prescribed by the gradient of the concentration, that is to say chiefly in the lateral direction outward into the cladding. This process leads to a change in the refractive index profile that influences the loss.

[0045] Since the concentration of the dopant at the core/cladding boundary decreases as a consequence of the diffusion, the image contrast is reduced at the splice point, that is to say the pair of lines 21' representing the fiber core appear to be less dark in the shadow image produced, in particular in the middle 25 of the splice, than outside the heating zone 26, for example (see figure 8). The change $\Delta\rho_{x/y}$, caused by diffusion, in the dopant concentration on

the z-axis thereby approximately follows the bell-shaped curve illustrated in the right-hand upper part of Fig. 8.

[0046] In order to obtain the distribution of the refractive index n(r,z) at the splice, the basic distribution $n_0(r,z_0)$ is compressed or stretched in the lateral direction with the aid of a parameter $S_{x/y}(z) = f(K_{x/y}(z))$ dependent on the ratio

$$K_{x/y}(z): = H_{x/y}(z)/H_{x/y}(z_0) \qquad (3)$$

$H_{x/y}(z)$:brightness/intensity of the core boundary at a point z in the region of the splice

$H_{x/y}(z_0)$: brightness/intensity of the core boundary at a point z_0 outside the heating zone,

such that the distribution n(r) being sought exhibits the profile, illustrated in the right-hand lower part of figure 8, on the z-axis. The ratio $K_{x/y}(z)$ can also serve approximately as a parameter $S_{x/y}(z)$.

[0047] If the core is not to be discerned in the shadow images (simple optical system), it is possible to deduce the level of the diffusion and thus the stretch/compression factor by measuring the splicing temperature (for example directly or indirectly via the brightness of the heated fiber) or from the heating temperature set at the splicer.

Ascertaining the initial field distribution

[0048] The initial field distribution $\overline{E}_0(\overline{r})$ featuring in the calculation of the splice loss corresponds to the spatial dependence, derived from the basic distribution $n_0(\overline{r})$ of the refractive index for a given wavelength and the associated spatial region, of the electric field of a mode that can be propagated in the glass fiber (for example fundamental mode LP_{01} of a monomode glass fiber). Methods for calculating the field distribution from a prescribed spatial distribution of the refractive index are known, for example, from Siemens Forschungs- und Entwicklungsbreicht, Vol. 4, No. 3, 1985, Pages 89-96, and Journal of Lightwave Technology, Vol. 12, No. 3, March 1995, pages 487-494.

Calculating the final field distribution

[0049] The initial field distribution $\overline{E}_0(\overline{r})$, assigned to the mode that can be propagated, in a first spatial region enclosing the fiber core and situated upstream of the splice is used to calculate the spatial dependence, termed the final field distribution $\overline{E}_n(\overline{r})$ below, of the electric field of the mode, propagating from the first spatial region via the splice, within a second spatial region situated downstream of the splice in the direction of propagation, by

means of one of the beam propagation methods (BPM) described in IEEE Photonics Technology Letters, Vol. 4, No. 2, February 1992, pages 148-151; Journal of Lightwave Technology, Vol. 10, No. 3, March 1992, pages 295-305; and IEEE Photonics Technology Letters, Vol. 5, No. 9, September 1993, Pages 1073-11076.

[0050] The BPM firstly requires the refractive index distribution at discrete points in space, which is subdivided, for example, into cuboids of equal size. The edge length of each cuboid can be 0.5 μm, for example, in the z-direction, and 0.25 μm in the x- and y-direction, in each case (see Fig. 9), all the cuboids with the same z-coordinate forming a spatial region denoted as a layer. Each cuboid is assumed to be homogeneous with reference to the refractive index, that is to say the refractive index does not change inside the respective cuboid.

[0051] Since the distribution of the refractive index cannot be determined from the above described measurements with the accuracy required for the BPM, the missing data points are determined by interpolation (for example, using splines). This can even be done straight away, since the refractive index changes only very little between two points in space which are still just resolved by the imaging system.

[0052] If the electric field $\overline{E}_0(x, y, z_0)$ (termed $\overline{E}(z_0)$ below) describing a mode that can be propagated in the glass fiber and derived from the basic distribution $n_0(\overline{r})$ is present at the centers of the cuboid end faces of the first layer (symbolized by black points in Fig. 9), the BPM uses this initial field distribution and the refractive indices of the first layer to calculate the electric field $\overline{E}(x, y, z_0 + \Delta z)$ between the first and second layers and again, therefrom, the electric field $\overline{E}(x, y, z_0 + 2\Delta z)$ between the second and third layers. If the method is continued iteratively, the BPM finally supplies the electric field $\overline{E}_n(x, y, z_0 + n\Delta z)$ (termed $\overline{E}(z_n)$ below), representing the final field distribution, at the end surface of the last layer.

[0053] Numerous variants of the BPM exist, the desired accuracy, the required computational outlay and the tolerable computer time determining the selection of the method to be applied. Thus, the computational outlay and therefore the computer time can be reduced for a given computer power

- by using a method operating with the aid of a slowly varying envelope approximation (splice geometry deviates only negligibly from that of the undisturbed fiber),
- by applying a scalar BPM (weak transverse mode coupling), or
- by reducing the three-dimensional distribution of the refractive index, for example with the aid of the method of the effective index, to a two-dimensional problem (simple splice geometry).

Calculating the splice loss

[0054] The splice loss can be calculated from the initial field distribution $\overline{E}(z_0)$ of the final distribution $\overline{E}(z_n)$ or the corresponding intensities $I(z_0)$ and $I(z_n)$, respectively, by means of

$$L_{[dB]} = 10\log_{10}\left(\frac{I(z_0)}{I(z_n)}\right) \qquad (4)$$

The above formula assumes that $E(z_n)$ describes a mode that propagates even over relatively large distances in the fiber. If the final field distribution $\overline{E}(z_n)$ also includes amounts of modes that cannot propagate, it is necessary at first to decompose $\overline{E}(z_n)$ in accordance with the equation (4), v denoting the order of the highest mode that can still propagate, and w denoting the order of the highest mode contained in $\overline{E}(z_n)$.

$$\overline{E}(z_n) = \sum_{i=0}^{v} \overline{E}_i(z_n) + \sum_{j=v+1}^{w} \overline{E}_j(z_n) \qquad (5)$$

Consequently, the variable $\Sigma\,\overline{E}_i(z_n)$ represents the total field distribution of the modes that can propagate, and $\Sigma\,\overline{E}_j(z_n)$ represents the total field distribution of the modes that cannot propagate, the intensity $I(z_n)$ derived only from $\Sigma\,\overline{E}_i(z_n)$ featuring in the calculation of the loss.

[0055] The determination of the final field distribution from the initial field distribution requires a high computational outlay, and so it is possible, depending on the performance of the processor built into the splicer, for a relatively long time to elapse before the splice loss is indicated on the display screen. This can be avoided by no longer calculating the final field distribution directly in the splicer, but doing so in advance at the manufacturers. T here, the parameters relevant to the loss are determined from a large number of recorded splice geometries and the loss values calculated using a powerful processor. These parameters need not necessarily have a physical analogy (for example core offset, etc). Methods for determining such parameters are known from statistics or physics by the designation of main components or factor analysis or Karhunen-Loeve decomposition. The functional relationship of the parameters with the calculated loss defines a characteristic diagram which is stored in each splicer. The function of the splicer then reduces to using the parameters to classify the splice produced and reading of the assigned loss from the characteristic diagram.

Clean Version of Amended Application

SI01-030

Patent Claims:

11. A method for determining the loss of a splice connecting two optical waveguides by executing the following steps:

a) determining or describing a first spatial distribution of the refractive index ($n_0(\vec{r})$) inside a first spatial region, not influenced by the splice, of a first optical waveguide,

b) determining a second spatial distribution ($n(\vec{r})$) of the refractive index in the region of the splice,

c) deriving a first field function ($\vec{E}(z_0)$) from the first spatial distribution ($n_0(\vec{r})$) of the refractive index, the first field function ($\vec{E}(z_0)$) describing the spatial dependence of the electric field of a mode that can propagate in the waveguides,

d) calculating a second field function ($\vec{E}(z_n)$) from the first field function ($\vec{E}(z_0)$) and the second spatial distribution of the refractive index ($n(\vec{r})$), the second field function ($\vec{E}(z_n)$) describing the spatial dependence of the electric field, the mode propagating from the first spatial region via the splice, within a second spatial region, not influenced by the splice, of the second optical waveguide,

e) calculating a first intensity ($I(z_0)$) and a second intensity ($I(z_n)$) from the assigned field functions ($\vec{E}(z_0)$, $\vec{E}(z_n)$), and

f) calculating the loss (L) of the splice occurring as a function of the ratio of the two intensities ($I(z_0)$, $I(z_n)$).

12. The method according to claim 11, wherein the loss (L) of the splice is calculated in accordance with the relationship

$$L_{[dB]} = 10\log_{10}\left(\frac{I(z_0)}{I(z_n)}\right)$$

13. The method according to claim 11, wherein the second spatial distribution ($n(\vec{r})$) of the refractive index is determined by transverse irradiation of the splice with light and

evaluation of the intensity distribution generated downstream of the splice in the beam direction, or of the shadow image.

14. The method according to claim 12, wherein the second spatial distribution ($n(\vec{r})$) of the refractive index is determined by transverse irradiation of the splice with light and evaluation of the intensity distribution generated downstream of the splice in the beam direction, or of the shadow image.

15. The method according to claim 13, wherein the waveguides and the splice are trans-illuminated from two directions enclosing an angle of $\alpha \neq 180°$, and in that the transmitted radiation is projected in each case by means of an optical system onto a sensor or detector element defining a plane.

16. The method according to claim 14, wherein the waveguides and the splice are trans-illuminated from two directions enclosing an angle of $\alpha \neq 180°$, and in that the transmitted radiation is projected in each case by means of an optical system onto a sensor or detector element defining a plane.

17. The method according to claim 15, wherein the planes respectively defined by the sensor or detector element enclose an angle of approximately 90°.

18. The method according to claim 16, wherein the planes respectively defined by the sensor or detector element (16, 17) enclose an angle of approximately 90°.

19. The method according to claim 13, wherein an offset of the center of the optically-conducting core of the waveguides in the region of the splice is determined at least in a first spatial direction from the shadow image, in that the first spatial distribution of the refractive index corresponding to the offset of the light-conducting core is displaced in the corresponding spatial direction, and the modified first spatial distribution of the refractive index represents the second spatial distribution of the refractive index.

20. The method according to claim 14, wherein an offset of the center of the optically-conducting core of the waveguides in the region of the splice is determined at least in a first spatial direction from the shadow image, in that the first spatial distribution of the refractive index corresponding to the offset of the light-conducting core is displaced in the corresponding spatial direction, and in that the modified first spatial distribution of the refractive index represents the second spatial distribution of the refractive index.

21. The method according to claim 19, wherein the offset of the optically-conducting core is derived from the offset of the center line of the outer contour of the waveguides in the region of the splice.

22. The method according to claim 20, wherein the offset of the optically-conducting core is derived from the offset of the center line of the outer contour of the waveguides in the region of the splice.

23. The method according to claim 13, wherein a tapering or expansion of the light-conducting core of the waveguides in the region of the splice is determined at least in a first spatial direction from the shadow image, in that the first spatial distribution of the refractive index is compressed or stretched in the corresponding spatial direction by a factor proportional to the ratio $[d_{x/y}(z)]/[d_{x/y}(z_0)]$, $d_{x/y}(z_0)$ denoting the width of the core at a point z_0, not influenced by the splice, of the waveguides, and $d_{x/y}(z)$ denoting the width of the core at a point z lying in the region of the splice, and in that the correspondingly compressed or elongated first spatial distribution of the refractive index represents the second spatial distribution of the refractive index.

24. The method according to claim 14, wherein a tapering or expansion of the light-conducting core of the waveguides in the region of the splice is determined at least in a first spatial direction from the shadow image, in that the first spatial distribution of the refractive index is compressed or stretched in the corresponding spatial direction by a factor

proportional to the ratio $[d_{x/y}(z)]/[d_{x/y}(z_0)]$, $d_{x/y}(z_0)$ denoting the width of the core at a point z_0, not influenced by the splice, of the waveguides, and $d_{x/y}(z)$ denoting the width of the core at a point z lying in the region of the splice, and in that the correspondingly compressed or elongated first spatial distribution of the refractive index represents the second spatial distribution of the refractive index.

25. The method according to claim 23, wherein the tapering or expansion or of the light-guiding core is derived respectively from the tapering or expansion of the outer contour of the waveguides in the region of the splice.

26. The method according to claim 24, wherein the tapering or expansion or of the light-guiding core is derived respectively from the tapering or expansion of the outer contour of the waveguides in the region of the splice.

27. The method according to claim 13, wherein the brightness of an edge delimiting the light-guiding core of the cladding of the waveguide is of the measured in at least one of the two shadow images in the region of the splice and in a second region not influenced by the splice, in that the first spatial distribution of the refractive index is spatially modified in accordance with a factor dependent on the measured brightnesses, and in that the modified first spatial distribution of the refractive index represents the second spatial distribution of the refractive index.

28. The method according to claim 14, wherein the brightness of an edge delimiting the light-guiding core of the cladding of the waveguide is of the measured in at least one of the two shadow images in the region of the splice and in a second region not influenced by the splice, in that the first spatial distribution of the refractive index is spatially modified in accordance with a factor dependent on the measured brightnesses, and in that the modified first spatial distribution of the refractive index represents the second spatial distribution of the refractive index.

Abstract of the Invention

The invention relates to methods for determining the attenuation of a splice connecting two optical waveguides. Methods for assessing the quality of the splice provide high precision results only when the dimensions of the light-conducting fiber, i.e., the spatial distribution of the refractive index which determines the attenuation behavior, are used in the calculation of the attenuation. The dimensions of the splice are measured in a three-dimensional manner by optical systems, and the spatial distribution of the refractive index of the splice is derived therefrom. The field distribution corresponding to a mode that is capable of propagating in the fiber is fixed within a first spatial region situated in front of the splice in the beam direction; and the field distribution of this mode is determined within a second spatial region situated behind the splice in a beam direction while taking into consideration the spatial distribution of the refractive index of the splice. The splice attenuation is calculated from the intensity values assigned to both field distributions

Description

CALCULATING SPLICE LOSS BY GEOMETRIC MEASUREMENT

1. Introduction

The method known as "thermal splicing" can be used to interconnect both monomode and multimode glass fibers and glass fiber strips in a bonded, low-loss and permanent fashion. Since the costs of constructing an optical waveguide cable network are not inconsiderably influenced by splicing as a work step that is frequently to be carried out, convenient devices which can also be used on site under difficult conditions have been developed which execute all the steps required for welding glass fibers in a largely fully automatic fashion (see [1], for example). The loss in the splice junction produced in such a device is a function, inter alia, of the exact alignment of the optically conducting fiber cores, the quality of the fiber end faces (roughness, angle of fracture, etc) and of the welding parameters (welding time, welding current) selected by the operator or described by the respective control program.

2. Prior art

Disturbances in the geometry of the optically conducting fiber core are decisive for the magnitude of the loss in the splice produced. The loss caused, in particular, by a core offset, bending of the core or widening or tapering of the core can be determined, for example, by means of a transmission measurement and the use of a bending coupler (LID system) installed in the splicer. In this case, light is coupled into the glass fiber upstream of the splice point, and coupled out again downstream of the splice point. The intensity of the light transmitted from one glass fiber into the other glass fiber via the splice is then a measure of

the loss. This measurement method cannot be applied, however, when an excessively thick or dark-colored fiber coating prevents light from being coupled into and out of the fiber core.

The method disclosed in [2] for determining the splice loss is based on the optical detection of the core offset, the oblique position of the fiber cores and the core bending in the region of the splice point. An empirically determined formula describes the functional dependence of the loss on the said parameters. Since the method does not require light to be coupled into and out of the fiber core, it can always be applied independently of the light-passing capability of the fiber coating. However, it supplies reliable loss values only when the previously named parameters alone determine the loss of the splice. However, this is not always the case, particularly with wrongly set welding parameters or high losses.

3. Subject matter, goals and advantages of the invention

The subject matter of the invention is a method for determining the loss of a splice connecting two optical waveguides. The term "splice" in this case denotes that bonded connection, in particular produced by thermal fusing/welding, between at least two optically conducting structures or elements, that is to say, in particular, the connection between glass fibers, glass fiber strips/ glass fiber bundles or the connection between a glass fiber or a glass fiber strip and an active or passive optical component.

The method is intended to enable the user to determine the loss in the splice produced, doing so with high accuracy while taking account of all the parameters substantially influencing the loss. This object is achieved by means of a method having the features

specified in patent claim 1. The dependent claims relate to advantageous embodiments and developments of the method.

The proposed method can be applied straight away in a modern splicer, since all that is needed is to adapt its software appropriately. The method is distinguished, furthermore, by the following properties:

- the achievable accuracy of the determination of loss is limited essentially only by the quality of the optical system serving to visualize the fiber core, and the performance of the processor executing the field calculation;
- the loss in the splice can be determined as a function of direction;
- comparatively thick and/or darkly colored fiber coatings cannot impair the measurement;
- the splice loss can be calculated for any desired operating wavelength, and
- the method permits simple adaptation to the respective requirements (for example high accuracy, fast measurement).

4. Drawings

The invention is explained in more detail below with the aid of drawings, in which:

Figure 1 shows the schematic structure of a modern thermal splicer operating largely fully automatically;

Figure 2 shows the relative position of the ends of two optical fibers that are to be connected;

a) after being brought together and coarsely positioned;

b) after being aligned with reference to their outer contours, and

c) after being aligned with reference to their optically conducting fiber cores;

Figure 3 shows the schematic structure of a glass fiber, and the profile n(r) of the refractive index in the plane oriented perpendicular to the fiber longitudinal axis;

Figure 4 shows the intensity distribution ("shadow image" of the glass fiber) produced in the case of transverse transillumination of a glass fiber, by means of an imaging optical system in the sensor plane of a CCD camera;

Figure 5 shows the shadow image of the glass fiber whose core has a lateral offset in the region of the splice;

Figure 6 shows the shadow image of a glass fiber whose core is bent in the region of the splice;

Figure 7 shows the shadow image of a glass fiber whose core is expanded/compressed in the region of the splice;

Figure 8 shows the shadow image of a glass fiber in the case of which, because of the diffusion of the dopant atoms, the pair of lines defining the core exhibit a lesser brightness or a lesser contrast in the region of the splice than outside the heating zone; and

Figure 9 shows the subdivision into cuboids and layers of the space on which the method of field calculation is based and containing the fiber core.

5. Description of the exemplary embodiments

The splicer illustrated only schematically in figure 1 permits optical fibers to be welded in a largely fully automatic fashion. The bonded connection of the optical fibers that is produced with the aid of an arc (electric glow discharge) struck between two electrodes, which is denoted below as "splice" for short, is free of inclusions, the loss caused by the

splice being on average approximately L = 0.02 -0.03 dB (identical standard monomode glass fibers).

The connection of the monomode or multimode glass fibers consisting in each case of a core (refractive index n_{core}), a cladding (refractive index $n_{cladding} < n_{core}$) and a coating of one or more layers is usually performed by executing the following method steps:

a) preparing the fiber ends 1/2, that is to say carefully removing the fiber coating, cleaning the fiber ends 1/2 and breaking the fibers in such a way that the fiber end faces are orientated approximately perpendicular to the fiber longitudinal axis (angle of fracture < 0.8°; typically 0.5°);

b) fixing the fiber ends 1/2 in the holders of the splicer;

c) bringing the fiber ends 1/2 together and aligning them by means of high-precision positioning units 3/4/5 by using the LID system 6/7 (Local Injection and Detection) and/or by video image evaluation;

d) cleaning the fiber end faces by briefly heating the fiber ends 1/2;

e) feeding the fiber ends 1/2 and fusing them by striking an electric arc between two electrodes 8/9 arranged in the region of the fiber ends 1/2, and

f) checking the quality of the splice (measuring the splice loss, checking the tensile strength).

Whereas the method steps a) and b) must be executed by the operator, that is to say still have to be done manually, the method steps specified under c) to f) and mentioned further in [1], in particular the determination of the angle of fracture, the quality and the level of contamination of the fiber end faces run under program control in the splicer.

The splicer is equipped with the following components and elements in order to carry out these method steps:

- three positioning units 3/4/5 for independently displacing the fiber ends 1/2, respectively guided in V grooves, in three orthogonal spatial directions (x-, y- and z-axis ≙ fiber longitudinal axis),
- a control unit 10 for driving the actuating elements (positioning motors, piezoelectric actuators) of the positioning units 3/4/5,
- a transmission measuring device consisting of an optical transmitter 6 (light-emitting diode, bending coupler) and an optical receiver 7 (bending coupler, photodiode, amplifier) (LID system, see [1], for example),
- two optical systems for projecting the outer contours or the profile of the two fiber ends 1/2 into two planes (x/z- or y/z-plane) orientated orthogonally relative to one another, the optical systems respectively have a light source 11/12 (light-emitting diode), an imaging optical system 13/14 and a CCD camera 16/17 which is connected to the video evaluating unit 15 and defines the x/z or the y/z sensor plane,
- a heat source for heating the fiber ends 1/2 to the melting temperature, situated in the region between approximately 1600-2000°C, the supply of heat being performed in the exemplary embodiment shown by means of a glow discharge produced between two electrodes 8/9 and controlled by the unit 18,
- a central controller 19 which is connected on the input side to the video evaluating unit 15 and executes and monitors all the steps required for splicing in accordance with the selected program, and
- an LCD monitor (not illustrated).

After the glass fibers have been inserted into the holder of the splicer, their ends 1/2 are not generally aligned opposite one another. As illustrated in figure

2 schematically in side view, both the outer contours of the fiber ends 1/2 and the fiber cores C1/C2 then do not necessarily exhibit a transverse offset δ_k or δ_c of the same size. The offset δ_k of the outer contours is now measured by evaluating the projections, recorded with the aid of the two CCD cameras 16/17, of the fiber ends 1/2 in the x/z-plane or the y/z-plane. Subsequently, the fiber ends 1/2 are displaced with the aid of the first positioning units 3/4/5, driven with the aid of the control unit 10, in a transverse direction, that is to say in the direction of the x- and y-axes until the outer contours of the fiber ends 1/2 are aligned, their transverse offset δ_k thus vanishing at least approximately ($\delta_{kx} \approx \delta_{ky} \approx 0$) both in the x- and in the y-directions. After this alignment, referred to as fine positioning, the fiber ends 1/2 are situated opposite one another, as illustrated in figure 2b. The core offset δ_c, caused by the eccentric position of the fiber cores C1/C2, which is still present is clearly to be seen.

In order to produce a splice with the lowest possible loss, the fiber ends 1/2 must therefore further be aligned with regard to their cores C1/C2, that is to say the core offset δ_c must be removed or at least minimized. This is performed by using the LID system, which feeds the IR radiation, emitted by a light-emitting diode on the transmitter 6, of wavelength $800 \text{ nm} \leq \lambda \leq 1600 \text{ nm}$, in particular $\lambda = 1300$ nm or $\lambda = 1550$ nm, into the left-hand glass fiber via the assigned bending coupler, and measures the intensity of the radiation, coupled from the left-hand fiber end 1 into the right-hand fiber end 2, by means of the optical receiver, consisting of a second bending coupler and a photodiode amplifier unit. The fiber ends 1/2 are displaced in this case in the transverse direction until the radiation intensity measured in the optical receiver 7 of the LID system reaches a maximum, the fiber ends 1/2 thereby assuming the position

illustrated in figure 2c (fiber cores C1/C2 in line and aligned in parallel with the z-axis; small contour offset corresponding to the corrected core offset δ_c).

Subsequently, the fiber ends 1/2 are heated by striking the electric arc between the electrodes 8/9, brought together and fused with one another. During this process, the LID system 6/7 continuously measures the light transmission via the splice point. If the intensity measured in the optical receiver 7 reaches a maximum, the optimum welding period is reached and the welding operation is automatically terminated. By applying this technique, referred to as automatic fusion time control, it is possible largely to compensate the effects caused by the state of the electrodes 8/9 (non-optimum spacing, wear, etc) and/or by environmental influences (moisture, air pressure, temperature), and which lead to a rise in splice loss.

Despite every care taken and the precision exercised during the preparation, alignment and bringing together of the glass fibers 1/2, it is not possible, as a rule, completely to avoid a residual offset of the fiber cores C1/C2, oblique positioning of the fiber longitudinal axes and/or of the fiber end faces, as well as an overtravel (the incipiently fused fiber ends are brought together and pushed into one another beyond the permissible extent). Depending on the extent/magnitude of these "faulty positions", it follows that in the region of the splice produced the geometry of the fiber core C1/C2 deviates more or less strongly from that of the undisturbed fiber. Since it is essentially only the fiber core that transports the light, disturbances in the core geometry in the region of the splice are chiefly responsible for the increase in the loss. Thus, methods for determining the quality of a splice can therefore supply results of high precision only when the core geometry, that is to say the spatial distribution of the refractive index $n(\vec{r})$

determining the loss response, at the splice point features in the calculation of the loss.

In the case of the proposed method, the splice geometry is detected in three dimensions by means of the optical systems 11 - 17 present in the splicer and therefrom the spatial distribution $n(\vec{r})$ of the refractive index that exactly describes the splice and its properties (that is to say also the loss) is derived. In detail, the determination of the splice loss requires the execution of the following steps, explained below in more detail:

- determining the splice geometry in three dimensions and calculating the spatial distribution $n(\vec{r})$ of the refractive index;
- ascertaining the field distribution ("initial field distribution" $\vec{E}(z_0)$) of a mode that can be propagated in the glass fiber (corresponding, for example, to the fundamental mode LP_{01} in what is termed a monomode glass fiber) inside a spatial region situated upstream/downstream of the splice in the beam direction;
- calculating the field distribution ("final field distribution" $\vec{E}(z_n)$) of this mode inside a spatial region situated downstream of the splice in the beam direction, and
- calculating the loss in the splice from the intensity values assigned to the two field distributions.

Detecting the splice geometry in three dimensions

A glass fiber serving to transport electromagnetic radiation and denoted in figure 3 by 20 consists, for example, of a Ge-doped SiO_2 core 21 (n_{core} = 1.48), and SiO_2 cladding 22 ($n_{cladding}$ = 1.46) concentrically sheathing the core 21, and on a plastic coating 23 that protects a core 21 and cladding 22 against external mechanical, thermal and chemical actions and is usually

of colored finish and, if appropriate, also provided with a ring marking. In the case of a monomode glass fiber 20, the core glass diameter is typically ϕ_{core} = 9 µm, while the cladding glass diameter is typically $\phi_{cladding}$ = 125 µm.

Since the concentration of the dopant in the glass fiber 20 has a constant value on the fiber longitudinal axis OA, and exhibits in the plane orthogonal thereto, for example, the profile illustrated in the right-hand part of figure 3, the spatial distribution of the refractive index $n(\overline{r})$ is also radially symmetrical with reference to the fiber longitudinal axis OA ($n(\overline{r}) = n(r,z=z_0)$). Because of the already mentioned effects (offset of the fiber core, oblique position of the fiber end faces, etc before the splicing), the spatial distribution of the refractive index $n(\overline{r})$ in the region of the splice can differ substantially in some circumstances from the refractive index distribution $n_0(\overline{r})$ of the undisturbed glass fiber. As already explained, it is essentially only the deformation of the optically conducting regions, that is to say the fiber core 21, that is responsible for the loss in intensity at the splice point. Consequently, to calculate the loss it suffices to know the spatial distribution $n(\overline{r})$ of the refractive index inside a volume containing the core 21 and extending, for example, only 20 - 40 µm in the transverse direction (x/y-plane).

Recording images of the splice

Figure 4 shows the intensity distribution generated by the imaging optical system 14 on the sensor surface 17', defining the x/z-plane, of the CCD camera 17, when a glass fiber 20 stripped of its protective coating 22 is transilluminated by activating the light source 12 in the transverse direction (x-direction). Clearly in evidence are the outer contours 22' (outer edge of the

fiber cladding 22) of the glass fiber 20, the two dark zones 24/24' caused by the cylinder lens effect, and the image of the fiber core 21 (pair of lines 21'). A corresponding shadow image is produced by the system, comprising the light source 11 and the imaging optical system 13, on the sensor surface, defining the x/z-plane, of the CCD camera 16. The two intensity distributions are fed via the video evaluating unit 15 to the controller 19, which is equipped with a powerful microprocessor, and stored there in digital form.

Direct calculation of distribution $n(\overline{r})$ of the refractive index from the image of the splice

If the optical systems of the splicer have a sufficiently high resolution, the spatial distribution of the refractive index $n(\overline{r})$ can be calculated directly from the recorded images, for example with the aid of the method described in [3]. This does not require any additional information, although the distribution of the refractive index still requires to be standardized in some way. There are, however, the disadvantages of the necessary imaging optical system, which meets high demands and is therefore comparatively expensive, and of the expenditure, additionally required in the case of some methods, for generating interference images.

Deriving the distribution of the refractive index $n(\overline{r})$ from a basic distribution $n_0(\overline{r})$

In order to determine the spatial distribution of the refractive index $n(\overline{r})$ in the region of the splice, what is termed a basic distribution $n_0(\overline{r})$ of the refractive index is modified by means of suitable parameters obtained from the recorded images of the splice. The spatial distribution of the refractive index in the undisturbed glass fiber serves, in particular, as basic distribution $n_0(\overline{r})$. Said undisturbed glass fiber is known in the case of use of specific types of glass

fibers (standard fiber, dispersion-shifted fiber, erbium-doped fiber, etc), or it can be taken from the data sheet or supplied by the manufacturer upon request. If appropriate information is not available, the distribution $n_0(\vec{r})$ of the refractive index of the undisturbed fiber can be determined experimentally, for example by means of the method described in [4].

It is advantageous in practice for the spatial distribution, serving as basic distribution $n_0(\vec{r})$, of the refractive index of the undisturbed fiber to be determined in advance for the different, frequently used fiber types and to be stored in the splicer, if appropriate in parametric form. Since the glass fibers used in telecommunication are for the most part designed to be homogeneous in the direction of their longitudinal axis OA and to be rotationally symmetrical with reference to this axis OA, the distribution of the refractive index also has a corresponding symmetry, that is to say what is termed the refractive index profile $n(r, z_0)$ (r: lateral distance from the fiber longitudinal axis OA) describes the distribution of the refractive index completely.

The following examples explain the steps required to determine the distribution $n(\vec{r})$, featuring in the calculation of the loss, in the region of the splice by modifying a basic distribution $n_0(r)$. For the sake of clarity, the effects and mechanisms which act to increase loss and occur in practice simultaneously for the most part, are illustrated separately. The distribution $n_{\lambda 1}(\vec{r})$, determined for a wavelength $\lambda 1$, of the refractive index can be converted in this case with the aid of what is termed the Sellmaier series (see [5], for example) into the corresponding distribution $n_{\lambda 2}(\vec{r})$ in the case of another wavelength $\lambda 2$.

Offset of the fiber cores

In the ideal state, the core and cladding of the two interconnected glass fibers have the same axes of symmetry, which coincide with the z-axis, in the region of the splice, as well. However, because of incorrect positioning of at least one of the two glass fibers in advance of fusing (null alignment), offsetting of the cores which disturbs the light propagation and increases the loss occurs in the region of the splice point 25 (see figure 5). Consequently, in the intensity distributions produced by the imaging optical systems 13/14 on the sensor surfaces of the CCD cameras 16/17, respectively, of the splice point there is to be observed a lateral displacement, proportional to the offset, of the pairs of lines 21'/21", representing the respective cores, with reference to the z-axis, the curve describing the lateral distance x_m/y_m of the core centers from the z-axis showing the stepped profile illustrated schematically in the right-hand upper part of figure 5.

If the spatial distribution $n_0(\bar{r})$ of the refractive index of the undisturbed glass fiber (basic distribution) in a transverse direction has, for example, a stepped profile illustrated in the lower part of figure 4, the refractive index distribution $n(\bar{r})$ being sought, which approximates the real conditions, is calculated by modifying the basic distribution $n_0(\bar{r})$ in accordance with equation (1).

$$n(r,z) = n_0(r' + \Delta r,\ z) \qquad (1)$$

$\Delta r^2 = x_m^2(z) + y_m^2(z)$

x_m: lateral displacement of the core center in the x/z-plane

y_m: lateral displacement of the core center in the y/z-plane

The refractive index profile therefore changes on the z-axis in accordance with the right-hand lower part of figure 5.

The offset of the pair of lines 21'/21" representing the fiber core 21 with reference to a reference position situated preferably at the left-hand or right-hand edge of the image is measured in order to extract with high accuracy from the images the lateral distances $x_m(z)/y_m(z)$ of the fiber center from the z-axis illustrated in the shadow image. The correlation method described in [6], for example, can be applied for this purpose.

If the optical system of the splicer does not permit images/visualization of the fiber core 21, it can be assumed in a first approximation that the core 21 does not significantly change its position relative to the outer contour of the fiber during fusing. The lateral distance of the middle of the core from the z-axis illustrated in the shadow image then approximately corresponds to the lateral distance of the center of the fiber outer contour 22' from this axis.

Bending of the fiber core

Bending of the fiber core in the region of the splice comes about, for example, because of the eccentric position of at least one of the two cores inside the respective glass fiber and/or the nonparallelism of the mutually opposite fiber end faces in advance of fusing. The two imaging optical systems 13/14 of the splicer then respectively generate a shadow image on the splice which is illustrated schematically in the left-hand part of figure 6. Outside the heating zone 26, the center of the fiber core is to be situated below on the z-axis, but to be offset in the middle 25 of the splice by $\Delta x(z_s)$ or $\Delta y(z_s)$ in the lateral direction. The lateral distance $\Delta x(z)/\Delta y(z)$ of the core center

therefore changes on the z-axis in accordance with the function that is illustrated in the right-hand upper part of figure 6 and passes through a minimum in the middle 25 of the splice (coordinate z_s).

In order to obtain the spatial distribution, approximated to the real conditions, of the refractive index in the region of the splice, the basic distribution $n_0(r)$ is displaced in the lateral direction in accordance with the measured lateral distance $\Delta x(z)/\Delta y(z)$ of the core center from the z-axis. The right-hand lower part of figure 6 shows the profiles $n(r,z)$ of the refractive index that are assigned to the various z-values.

Change in the cross section of the fiber core

If the two glass fibers to be connected are compressed or drawn apart from one another during the splicing operation, this produces an expansion or tapering of the fiber core and the outer contour in the region of the splice, something which influences the loss. In the shadow image of the splice that is produced (see figure 7), the lines 21' which delimit the fiber core from the fiber cladding and run outside the splice point approximately parallel to the z-axis then exhibit a distance from one another which is increased/reduced by comparison with the undisturbed regions situated at the edge of the image. The right-hand upper part of figure 7 shows the functional dependence of the widening $\Delta d_{x/y}$ of the core diameter along the z-axis. The width $d_{x/y}(z_s)$ of the core is greatest in the middle 25 of the splice. The ratio $V_{x/y}(z)$ given by

$$V_{x/y}(z) := [d_{x/y}(z)]/[d_{x/y}(z_0)] \qquad (2)$$

$d_{x/y}(z)$: spacing of the pair of lines 21' at a point z in the region of the splice

$d_{x/y}(z_0)$: spacing of the pair of lines 21' at a point z_0 outside the heating zone

therefore defines a measure of the change in cross section of the fiber core.

In order to obtain the distribution of the refractive index at the splice point, the basic distribution $n_0(r)$ is compressed or stretched in accordance with the ratio $V_{x/y}(z)$ in the x/y-plane, such that, for example, the refractive index profile illustrated schematically in the right-hand lower part of figure 7 is obtained at different points on the z-axis.

If no high quality imaging system is available (core not visible in the shadow image), the change in cross section of the fiber core can be equated at least approximately to the change in cross section of the outer contour (not illustrated in figure 7). It therefore suffices to measure the fiber outer contours 22' in the respective shadow image, in order to determine the compression or expansion factor $V_{x/y}(z)$ that can be applied to the basic distribution.

Diffusion of the dopant in the region of the splice

During the heating of the glass fibers in the arc, the dopant responsible for the different refractive indices of core and cladding begin to migrate in the direction prescribed by the gradient of the concentration, that is to say chiefly in the lateral direction outward into the cladding. This process leads to a change in the refractive index profile that influences the loss.

Since the concentration of the dopant at the core/cladding boundary decreases as a consequence of the diffusion, the image contrast is reduced at the splice point, that is to say the pair of lines 21' representing the fiber core appear to be less dark in

the shadow image produced, in particular in the middle 25 of the splice, than outside the heating zone 26, for example (see figure 8). The change $\Delta\rho_{x/y}$, caused by diffusion, in the dopant concentration on the z-axis thereby approximately follows the bell-shaped curve illustrated in the right-hand upper part of figure 8.

In order to obtain the distribution of the refractive index $n(r,z)$ at the splice, the basic distribution $n_0(r,z_0)$ is compressed or stretched in the lateral direction with the aid of a parameter $S_{x/y}(z) = f(K_{x/y}(z))$ dependent on the ratio

$$K_{x/y}(z) : = H_{x/y}(z)/H_{x/y}(z_0) \qquad (3)$$

$H_{x/y}(z)$: brightness/intensity of the core boundary at a point z in the region of the splice

$H_{x/y}(z_0)$: brightness/intensity of the core boundary at a point z_0 outside the heating zone,

such that the distribution $n(r)$ being sought exhibits the profile, illustrated in the right-hand lower part of figure 8, on the z-axis. The ratio $K_{x/y}(z)$ can also serve approximately as a parameter $S_{x/y}(z)$.

If the core is not to be discerned in the shadow images (simple optical system), it is possible to deduce the level of the diffusion and thus the stretch/compression factor by measuring the splicing temperature (for example directly or indirectly via the brightness of the heated fiber) or from the heating temperature set at the splicer.

Ascertaining the initial field distribution

The initial field distribution $\overline{E}_0(\overline{r})$ featuring in the calculation of the splice loss corresponds to the spatial dependence, derived from the basic distribution $n_0(\overline{r})$ of the refractive index for a given wavelength

and the associated spatial region, of the electric field of a mode that can be propagated in the glass fiber (for example fundamental mode LP_{01} of a monomode glass fiber). Methods for calculating the field distribution from a prescribed spatial distribution of the refractive index are known, for example, from [7, 8].

Calculating the final field distribution

The initial field distribution $\vec{E}_0(\vec{r})$, assigned to the mode that can be propagated, in a first spatial region enclosing the fiber core and situated upstream of the splice is used to calculate the spatial dependence, termed the final field distribution $\vec{E}_n(\vec{r})$ below, of the electric field of the mode, propagating from the first spatial region via the splice, within a second spatial region situated downstream of the splice in the direction of propagation, by means of one of the beam propagation methods (BPM) described in [9 - 11].

The BPM firstly requires the refractive index distribution at discrete points in space, which is subdivided, for example, into cuboids of equal size. The edge length of each cuboid can be 0.5 µm, for example, in the z-direction, and 0.25 µm in the x- and y-direction, in each case (see figure 9), all the cuboids with the same z-coordinate forming a spatial region denoted as a layer. Each cuboid is assumed to be homogeneous with reference to the refractive index, that is to say the refractive index does not change inside the respective cuboid.

Since the distribution of the refractive index cannot be determined from the abovedescribed measurements with the accuracy required for the BPM, the missing data points are determined by interpolation (for example using splines). This can even be done straight away, since the refractive index changes only very little

between two points in space which are still just resolved by the imaging system.

If the electric field $\overline{E}_0(x, y, z_0)$ (termed $\overline{E}(z_0)$ below) describing a mode that can be propagated in the glass fiber and derived from the basic distribution $n_0(\overline{r})$ is present at the centers of the cuboid end faces of the first layer (symbolized by black points in figure 9), the BPM uses this initial field distribution and the refractive indices of the first layer to calculate the electric field $\overline{E}(x, y, z_0 + \Delta z)$ between the first and second layers and again, therefrom, the electric field $\overline{E}(x, y, z_0 + 2\Delta z)$ between the second and third layers. If the method is continued iteratively, the BPM finally supplies the electric field $\overline{E}_n(x, y, z_0 + n\Delta z)$ (termed $\overline{E}(z_n)$ below), representing the final field distribution, at the end surface of the last layer.

Numerous variants of the BPM exist, the desired accuracy, the required computational outlay and the tolerable computer time determining the selection of the method to be applied. Thus, the computational outlay and therefore the computer time can be reduced for a given computer power

- by using a method operating with the aid of a slowly varying envelope approximation (splice geometry deviates only negligibly from that of the undisturbed fiber),
- by applying a scalar BPM (weak transverse mode coupling), or
- by reducing the three-dimensional distribution of the refractive index, for example with the aid of the method of the effective index, to a two-dimensional problem (simple splice geometry).

Calculating the splice loss

The splice loss can be calculated from the initial field distribution $\overline{E}(z_0)$ of the final distribution $\overline{E}(z_n)$ or the corresponding intensities $I(z_0)$ and $I(z_n)$, respectively, by means of

$$L_{[dB]} = 10\log_{10}\left(\frac{I(z_0)}{I(z_n)}\right) \qquad (4)$$

The above formula assumes that $E(z_n)$ describes a mode that propagates even over relatively large distances in the fiber. If the final field distribution $\overline{E}(z_n)$ also includes amounts of modes that cannot propagate, it is necessary at first to decompose $\overline{E}(z_n)$ in accordance with the equation (4), v denoting the order of the highest mode that can still propagate, and w denoting the order of the highest mode contained in $\overline{E}(z_n)$.

$$\overline{E}(z_n) = \sum_{i=0}^{v} \overline{E}_i(z_n) + \sum_{j=v+1}^{w} \overline{E}_j(z_n) \qquad (5)$$

Consequently, the variable $\Sigma\overline{E}_i(z_n)$ represents the total field distribution of the modes that can propagate, and $\Sigma\overline{E}_j(z_n)$ represents the total field distribution of the modes that cannot propagate, the intensity $I(z_n)$ derived only from $\Sigma\overline{E}_i(z_n)$ featuring in the calculation of the loss.

The determination of the final field distribution from the initial field distribution requires a high computational outlay, and so it is possible, depending on the performance of the processor built into the splicer, for a relatively long time to elapse before the splice loss is indicated on the display screen. This can be avoided by no longer calculating the final field distribution directly in the splicer, but doing so in advance at the manufacturers. There, the

parameters relevant to the loss are determined from a large number of recorded splice geometries and the loss values calculated using a powerful processor. These parameters need not necessarily have a physical analogy (for example core offset, etc). Methods for determining such parameters are known from statistics or physics by the designation of main components or factor analysis or Karhunen-Loeve decomposition. The functional relationship of the parameters with the calculated loss defines a characteristic diagram which is stored in each splicer. The function of the splicer then reduces to using the parameters to classify the splice produced and reading of the assigned loss from the characteristic diagram.

6. Literature

[1] ICCS and Future- Link; catalog 1998; Siemens-Communication-Cable Networks; pages 107 - 116

[2] EP 0 326 988 B1

[3] D. Marcuse "Principles of optical fiber measurements", Acad. Pr., 1981, ISBN 0-12-470980-X; pages 150 - 165

[4] H.-G. Unger, "Optische Nachrichtentechnik", Hüthig, 1993, ISBN 3-7785-2261-2, pages 648 - 671

[5] Electronic Letters, Vol. 14, No. 11, May 1978; pages 326 - 328

[6] W. Lieber, Th. Eder "Verfahren zur Ausrichtung zweier Lichtwellenleiter-Faserenden und Einrichtung zur Durchführung des Verfahrens" ["Method for aligning two optical waveguide fiber ends and device for carrying out the method"], EP-Appl. 90109388.0, 17.05.1990

[7] Siemens Forschungs- und Entwicklungsbericht, Volume 14, No. 3, 1985; pages 89 - 96

[8] Journal of Lightwave Technology, Vol. 12, No. 3; pages 487 - 494, March 1994

[9] IEEE Photonics Technology Letters, Vol. 4, No. 2, pages 148 - 151, February 1992

[10] Journal of Lightwave Technology, Vol. 10, No. 3; pages 295 - 305, March 1992

[11] IEEE Photonics Technology Letters, Vol. 5, No. 9; pages 1073 - 1076, September 1993

Patent claims

1. A method for determining the loss of a splice connecting two optical waveguides by executing the following steps:
   a) determining or describing a first spatial distribution of the refractive index ($n_0(\vec{r})$) inside a first spatial region, not influenced by the splice, of a first optical waveguide,
   b) determining a second spatial distribution ($n(\vec{r})$) of the refractive index in the region of the splice,
   c) deriving a first field function ($\vec{E}(z_0)$) from the first spatial distribution ($n_0(\vec{r})$) of the refractive index, the first field function ($\vec{E}(z_0)$) describing the spatial dependence of the electric field of a mode that can propagate in the waveguides,
   d) calculating a second field function ($\vec{E}(z_n)$) from the first field function ($\vec{E}(z_0)$) and the second spatial distribution of the refractive index ($n(\vec{r})$), the second field function ($\vec{E}(z_n)$) describing the spatial dependence of the electric field, the mode propagating from the first spatial region via the splice, within a second spatial region, not influenced by the splice, of the second optical waveguide,
   e) calculating a first intensity ($I(z_0)$) and a second intensity ($I(z_n)$) from the assigned field functions ($\vec{E}(z_0)$, $\vec{E}(z_n)$), and
   f) calculating the loss (L) of the splice occurring as a function of the ratio of the two intensities ($I(z_0)$, $I(z_n)$).

2. The method as claimed in claim 1, characterized in that the loss (L) of the splice is calculated in accordance with the relationship

$$L_{[dB]} = 10\log_{10}\left(\frac{I(z_0)}{I(z_n)}\right)$$

3. The method as claimed in claim 1 or 2, characterized in that the second spatial distribution ($n(\vec{r})$) of the refractive index is determined by transverse irradiation of the splice with light and evaluation of the intensity distribution generated downstream of the splice in the beam direction, or of the shadow image.

4. The method as claimed in claim 3, characterized in that the waveguides and the splice are transilluminated from two directions enclosing an angle of $\alpha \neq 180°$, and in that the transmitted radiation is projected in each case by means of an optical system (13, 14) onto a sensor or detector element (16, 17) defining a plane.

5. The method as claimed in claim 4, characterized in that the planes respectively defined by the sensor or detector element (16, 17) enclose an angle of approximately 90°.

6. The method as claimed in one of claims 3 to 5, characterized in that an offset of the center of the optically-conducting core of the waveguides in the region of the splice is determined at least in a first spatial direction from the shadow image, in that the first spatial distribution of the refractive index corresponding to the offset of the light-conducting core is displaced in the corresponding spatial direction, and in that the modified first spatial distribution of the refractive index represents the second spatial distribution of the refractive index.

7. The method as claimed in claim 6, characterized in that the offset of the optically-conducting core is derived from the offset of the center line of the outer contour of the waveguides in the region of the splice.

8. The method as claimed in one of claims 3 to 5, characterized in that a tapering or expansion of the light-conducting core of the waveguides in the region of the splice is determined at least in a first spatial direction from the shadow image, in that the first spatial distribution of the refractive index is compressed or stretched in the corresponding spatial direction by a factor proportional to the ratio $[d_{x/y}(z)]/[d_{x/y}(z_0)]$, $d_{x/y}(z_0)$ denoting the width of the core at a point z_0, not influenced by the splice, of the waveguides, and $d_{x/y}(z)$ denoting the width of the core at a point z lying in the region of the splice, and in that the correspondingly compressed or elongated first spatial distribution of the refractive index represents the second spatial distribution of the refractive index.

9. The method as claimed in claim 8, characterized in that the tapering or expansion or of the light-guiding core is derived respectively from the tapering or expansion of the outer contour of the waveguides in the region of the splice.

10. The method as claimed in one of claims 3 to 5, characterized in that the brightness of an edge delimiting the light-guiding core of the cladding of the waveguide is of the measured in at least one of the two shadow images in the region of the splice and in a second region not influenced by the splice, in that the first spatial distribution of the refractive index is spatially modified in accordance with a factor dependent on the measured

brightnesses, and in that the modified first spatial distribution of the refractive index represents the second spatial distribution of the refractive index.

Translation of Claims 11-28

Patent Claims:

11. A method for determining the loss of a splice connecting two optical waveguides by executing the following steps:

a) determining or describing a first spatial distribution of the refractive index ($n_0(\vec{r})$) inside a first spatial region, not influenced by the splice, of a first optical waveguide,

b) determining a second spatial distribution ($n(\vec{r})$) of the refractive index in the region of the splice,

c) deriving a first field function ($\vec{E}(z_0)$) from the first spatial distribution ($n_0(\vec{r})$) of the refractive index, the first field function ($\vec{E}(z_0)$) describing the spatial dependence of the electric field of a mode that can propagate in the waveguides,

d) calculating a second field function ($\vec{E}(z_n)$) from the first field function ($\vec{E}(z_0)$) and the second spatial distribution of the refractive index ($n(\vec{r})$), the second field function ($\vec{E}(z_n)$) describing the spatial dependence of the electric field, the mode propagating from the first spatial region via the splice, within a second spatial region, not influenced by the splice, of the second optical waveguide,

e) calculating a first intensity ($I(z_0)$) and a second intensity ($I(z_n)$) from the assigned field functions ($\vec{E}(z_0)$, $\vec{E}(z_n)$), and

f) calculating the loss (L) of the splice occurring as a function of the ratio of the two intensities ($I(z_0)$, $I(z_n)$).

12. The method as claimed in claim 11, characterized in that the loss (L) of the splice is calculated in accordance with the relationship

$$L_{[dB]} = 10\log_{10}\left(\frac{I(z_0)}{I(z_n)}\right)$$

13. The method as claimed in claim 11, characterized in that the second spatial distribution ($n(\vec{r})$) of the refractive index is determined by transverse irradiation of the splice with light and evaluation of the intensity distribution generated downstream of the splice in the beam direction, or of the shadow image.

14. The method as claimed in claim 12, characterized in that the second spatial distribution ($n(\vec{r})$) of the refractive index is determined by transverse irradiation of the

splice with light and evaluation of the intensity distribution generated downstream of the splice in the beam direction, or of the shadow image.

15. The method as claimed in claim 13, characterized in that the waveguides and the splice are trans-illuminated from two directions enclosing an angle of $\alpha \neq 180°$, and in that the transmitted radiation is projected in each case by means of an optical system (13, 14) onto a sensor or detector element (16, 17) defining a plane.

16. The method as claimed in claim 14, characterized in that the waveguides and the splice are trans-illuminated from two directions enclosing an angle of $\alpha \neq 180°$, and in that the transmitted radiation is projected in each case by means of an optical system (13, 14) onto a sensor or detector element (16, 17) defining a plane.

17. The method as claimed in claim 15, characterized in that the planes respectively defined by the sensor or detector element (16, 17) enclose an angle of approximately 90°.

18. The method as claimed in claim 16, characterized in that the planes respectively defined by the sensor or detector element (16, 17) enclose an angle of approximately 90°.

19. The method as claimed in one of claims 13, characterized in that an offset of the center of the optically-conducting core of the waveguides in the region of the splice is determined at least in a first spatial direction from the shadow image, in that the first spatial distribution of the refractive index corresponding to the offset of the light-conducting core is displaced in the corresponding spatial direction, and in that the modified first spatial distribution of the refractive index represents the second spatial distribution of the refractive index.

20. The method as claimed in one of claims 14, characterized in that an offset of the center of the optically-conducting core of the waveguides in the region of the splice is determined at least in a first spatial direction from the shadow image, in that the first spatial distribution of the refractive index corresponding to the offset of the light-conducting core is displaced in the corresponding spatial direction, and in that the modified first spatial distribution of the refractive index represents the second spatial distribution of the refractive index.

21. The method as claimed in claim 19, characterized in that the offset of the optically-conducting core is derived from the offset of the center line of the outer contour of the waveguides in the region of the splice.

22. The method as claimed in claim 20, characterized in that the offset of the optically-conducting core is derived from the offset of the center line of the outer contour of the waveguides in the region of the splice.

Translation of Claims 11-28

23. The method as claimed in one of claims 13, characterized in that a tapering or expansion of the light-conducting core of the waveguides in the region of the splice is determined at least in a first spatial direction from the shadow image, in that the first spatial distribution of the refractive index is compressed or stretched in the corresponding spatial direction by a factor proportional to the ratio $[d_{x/y}(z)]/[d_{x/y}(z_0)]$, $d_{x/y}(z_0)$ denoting the width of the core at a point z_0, not influenced by the splice, of the waveguides, and $d_{x/y}(z)$ denoting the width of the core at a point z lying in the region of the splice, and in that the correspondingly compressed or elongated first spatial distribution of the refractive index represents the second spatial distribution of the refractive index.

24. The method as claimed in one of claims 14, characterized in that a tapering or expansion of the light-conducting core of the waveguides in the region of the splice is determined at least in a first spatial direction from the shadow image, in that the first spatial distribution of the refractive index is compressed or stretched in the corresponding spatial direction by a factor proportional to the ratio $[d_{x/y}(z)]/[d_{x/y}(z_0)]$, $d_{x/y}(z_0)$ denoting the width of the core at a point z_0, not influenced by the splice, of the waveguides, and $d_{x/y}(z)$ denoting the width of the core at a point z lying in the region of the splice, and in that the correspondingly compressed or elongated first spatial distribution of the refractive index represents the second spatial distribution of the refractive index.

25. The method as claimed in claim 23, characterized in that the tapering or expansion or of the light-guiding core is derived respectively from the tapering or expansion of the outer contour of the waveguides in the region of the splice.

26. The method as claimed in claim 24, characterized in that the tapering or expansion or of the light-guiding core is derived respectively from the tapering or expansion of the outer contour of the waveguides in the region of the splice.

27. The method as claimed in one of claims 13, characterized in that the brightness of an edge delimiting the light-guiding core of the cladding of the waveguide is of the measured in at least one of the two shadow images in the region of the splice and in a second region not influenced by the splice, in that the first spatial distribution of the refractive index is spatially modified in accordance with a factor dependent on the measured brightnesses, and in that the modified first spatial distribution of the refractive index represents the second spatial distribution of the refractive index.

28. The method as claimed in one of claims 14, characterized in that the brightness of an edge delimiting the light-guiding core of the cladding of the waveguide is of the measured in at least one of the two shadow images in the region of the splice and in a second region not influenced by the splice, in that the first spatial distribution of the refractive index is spatially modified in accordance with a factor dependent on the measured brightnesses, and in that the modified first spatial distribution of the refractive index represents the second spatial distribution of the refractive index.

(12) NACH DEM VERTRAG ÜBER DIE INTERNATIONALE ZUSAMMENARBEIT AUF DEM GEBIET DES PATENTWESENS (PCT) VERÖFFENTLICHTE INTERNATIONALE ANMELDUNG

BERICHTIGTE FASSUNG

(19) Weltorganisation für geistiges Eigentum
Internationales Büro

(43) Internationales Veröffentlichungsdatum
21. Dezember 2000 (21.12.2000)

PCT

(10) Internationale Veröffentlichungsnummer
WO 00/077550 A1

(51) Internationale Patentklassifikation⁷: G02B 6/255, G01M 11/00

(21) Internationales Aktenzeichen: PCT/DE00/02008

(22) Internationales Anmeldedatum: 16. Juni 2000 (16.06.2000)

(25) Einreichungssprache: Deutsch

(26) Veröffentlichungssprache: Deutsch

(30) Angaben zur Priorität:
199 27 583.1 16. Juni 1999 (16.06.1999) DE

(71) Anmelder *(für alle Bestimmungsstaaten mit Ausnahme von US)*: SCC SPECIAL COMMUNICATION CABLES GMBH & CO KG [DE/DE]; Postfach 70 03 09, D-81303 München (DE).

(72) Erfinder; und

(75) Erfinder/Anmelder *(nur für US)*: ZAMZOW, Bert [DE/DE]; Thalkirchner Strasse 182, D-81371 München (DE).

(74) Anwalt: VIERING, JENTSCHURA & PARTNER; Steinsdorfstrasse 6, D-80538 München (DE).

(81) Bestimmungsstaat *(national)*: US.

[Fortsetzung auf der nächsten Seite]

(54) Title: ~~CALCULATION OF THE ATTENUATION OF A SPLICE ACCORDING TO THE MEASUREMENT OF THE DIMENSIONS~~

(54) Bezeichnung: BERECHNUNG DER SPLEISSDÄMPFUNG NACH MESSUNG DER GEOMETRIE

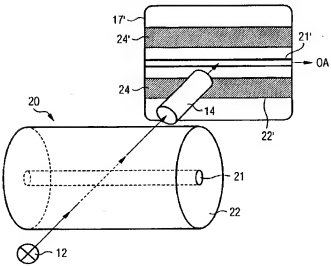

(57) Abstract: The assessment of the quality of a splice provides high-precision results only when the dimensions of the light-conducting fiber core, i.e. the spatial distribution of the refractive index, said distribution determining the attenuation behavior, in the area of the splice, are used in the calculation of the attenuation. As a result, the dimensions of the splice are measured in a three-dimensional manner by optical systems (12, 14), and the spatial distribution of the refractive index on the splice is derived therefrom. The field distribution corresponding to a mode that is capable of propagating in the glass fiber is fixed within a first spatial region situated in front of the splice in the beam direction. In addition, the field distribution of this mode is determined within a second spatial region situated behind the splice in a beam direction while taking into consideration the spatial distribution of the refractive index on the splice, and the splice attenuation is calculated from the intensity values assigned to both field distributions.

[Fortsetzung auf der nächsten Seite]

WO 00/077550 A1

FIG 1

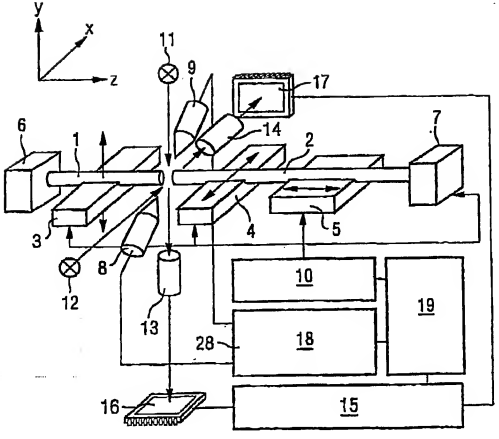

FIG 2A

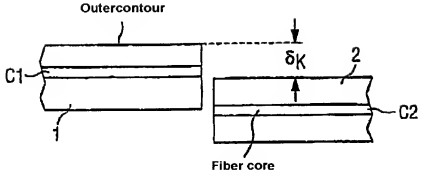

FIG 2B

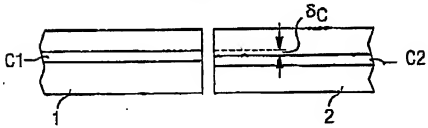

FIG 2C

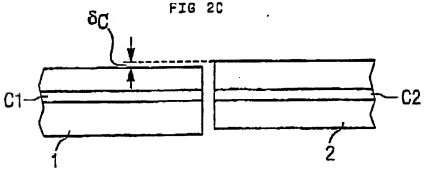

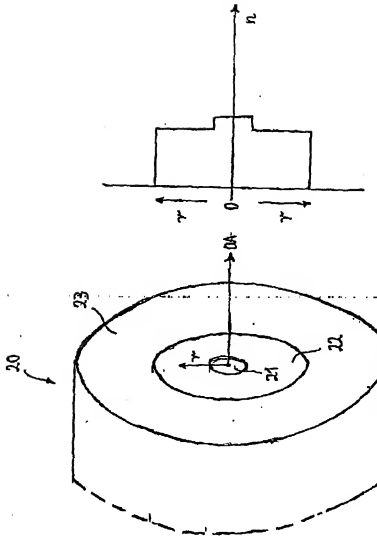

FIG 3

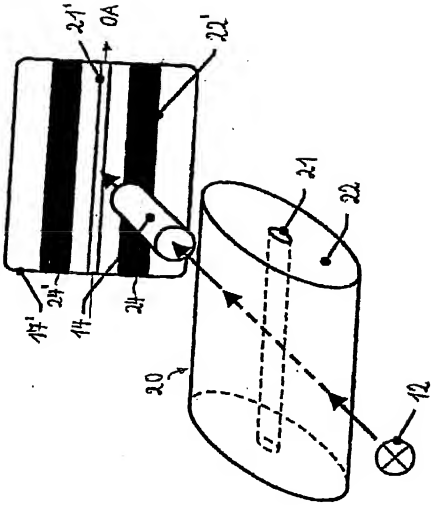

FIG 4

FIG 5

10018863

FIG 6

FIG 7

FIG 8

FIG 8

DECLARATION IN ORIGINAL APPLICATION **U.S. Attorney Docket No.: SI01-030**

As a below named inventor, I declare that:

My residence, Post Office address and citizenship are as stated below next to my name.

I believe I am the original, first and sole inventor (if only one name is listed below) or an original, first and joint inventor (if plural names are listed below) of the subject matter which is claimed and for which a patent is sought on the invention entitled **BERECHNUNG DER SPLEISSDÄMPFUNG NACH MESSUNG DER GEOMETRIE (METHODS FOR DETERMINING THE ATTENUATION OF A SPLICE THAT CONNECTS TWO OPTICAL WAVEGUIDES)**.

The specification of which (check only one item below):

[X] is attached hereto

[ ] was filed as United States Application Serial No. on and was amended on (if applicable)

[ ] was filed as PCT international application number , on , and was amended under PCT Article 19 on (if applicable).

I hereby state that I have reviewed and understand the contents of the above-identified specification, including the claims, as amended by any amendment referred to above.

I acknowledge the duty to disclose information which is material to the examination of this application in accordance with Title 37, Code of Federal Regulations, § 1.56.

I hereby claim foreign priority benefits under Title 35, United States Code, § 119(a)-(d) or 365(b) of any foreign application(s) for patent or inventor's certificate or 365(a) of any PCT international application which designated at least one country other than the Unites States, listed below and have also identified below any foreign application for patent or inventor's certificate, on the same subject matter, having a filing date before that of the application on which priority is claimed:

☒ **Country:** Germany **Application No.:** 199 27 583.1 **Filing Date:** 6/16/99

☐ **NONE**

I hereby claim the benefit under Title 35 United States Code § 119(e) and § 120 of any United States application(s) or 365(c) of any PCT international application designating the United States listed below and, insofar as the subject matter of each of the claims of this application is not disclosed in the prior United States application in the manner provided by the first paragraph of Title 35 United States Code § 112, I acknowledge the duty to disclose material information as defined in Title 37 Code of Federal Regulations, § 1.56 which occurred between the filing date of the prior application and the national or PCT international filing date of this application:

☐	**Provisional No.:**	**Filed:**	**Status:**
☒	**Application No.:**	**Filed:**	**Status:**
	PCT Application No: PCT/DE00/02008	**Filed:** 6/16/00	**Status:** filed

☐ **NONE**

DECLARATION IN ORIGINAL APPLICATION **U.S. Attorney Docket No.: SI01-030**

I hereby declare that all statements made herein of my own knowledge are true and that all statements made on information and belief are believed to be true; and further that these statements were made with the knowledge that willful false statements and the like so made are punishable by fine or imprisonment, or both, under Section 1001 of Title 18 of the United States Code and that such willful false statements may jeopardize the validity of the application or any patent issued thereon.

Full Name of Inventor: Bert Zamzow

Resident Address: Graffring 14, 44795 Bochum, Germany
Post Office Address: same

Citizenship: Germany

DATE: DEC-13-2001 X Bert Zamzow
Bert Zamzow